Received: 20 March 2022 | Revised: 24 June 2022 | Accepted: 27 June 2022

DOI: 10.1002/esp.5441

RESEARCH ARTICLE

ESPL WILEY

How do large wildfires impact sediment redistribution over multiple decades?

Dante Follmi[1] | Jantiene Baartman[1] | Akli Benali[2] | Joao Pedro Nunes[1,3]

[1]Soil Physics and Land Management Group, Wageningen University, Wageningen, The Netherlands

[2]Forest Research Centre, School of Agriculture, University of Lisbon, Lisbon, Portugal

[3]CE3C: Centre for Ecology, Evolution and Environmental Changes, School of Science, University of Lisbon, Lisbon, Portugal

Correspondence
Dr. ir. Jantiene EM Baartman, Soil Physics and Land Management Group (SLM), Wageningen University, PO Box 47, Wageningen 6700 AA, The Netherlands.
Email: jantiene.baartman@wur.nl

Funding information
cE3c research center, Grant/Award Number: UIDB/00329/2020; Erasmus+ travel fellowship; Portuguese Foundation for Science and Technology, Grant/Award Numbers: FRISCO project (PCIF/MPG/0044/2018), individual grant to A Benali (CEECIND/03799/2018/C, individual grant to JP Nunes (IF/00586/2015)

Abstract

Wildfires have become an increasing threat for Mediterranean ecosystems, due to increasing climate change-induced wildfire activity and changing land management practices. In addition to the initial risk, wildfires can alter the soil in various ways—depending on fire severity—and cause enhanced post-fire erosion. Usually, post-fire erosion studies focus on a short time window and lack the attention for sediment dynamics at larger spatial scales. Yet, these large spatial and temporal scales are fundamental for a better understanding of long-term destructive effects of multiple recurring wildfires on post-fire erosion processes and catchment sediment dynamics. In this study the landscape evolution model LAPSUS was used to simulate erosion and deposition in the 404 km^2 Águeda catchment in north-central Portugal over a 41-year (1979–2020) timespan, including eight wildfires each burning >1000 ha. To include variation in fire severity and its impact on the soil, four burn severity classes, represented by the difference normalized burn ratio (dNBR), were parameterized. Although model calibration was difficult due to lack of spatial and temporal measured data, the results show that long-term post-fire net erosion rates were significantly higher in the wildfire scenarios (5.95 ton ha^{-1} yr^{-1}) compared to those of a non-wildfire scenario (0.58 ton ha^{-1} yr^{-1}). Furthermore, erosion values increased with burn severity and multiple wildfires increased the overall catchment sediment build-up. Simulated erosion patterns showed great spatial variability, with large deposition and erosion rates inside streams. This variability made it difficult to identify land uses that were most sensitive for post-fire erosion, because some land uses were located in more erosion-sensitive areas (e.g. streams, gullies) or were more affected by high burn severity levels than others. Despite these limitations, LAPSUS performed well on addressing spatial sediment processes and can contribute to pre-fire management strategies, by identifying locations at risk of post-fire erosion.

KEYWORDS
burn severity, land and wildfire management, long-term modelling, post-fire erosion, sediment connectivity, wildfires

1 | INTRODUCTION

In recent decades, wildfires have become an increasing threat for Mediterranean ecosystems as a consequence of increasing frequency of weather conditions conducive for wildfires, which is likely to increase further due to climate change (Moriondo et al., 2006). This could lead to an increase in the number of years with high wildfire risk, an extension of the wildfire season, and an increase of extreme wildfire events. Subsequent impacts on vegetation and soils play an important role in land degradation (e.g. Malvar et al., 2011; Nunes, Naranjo Quintanilla, et al., 2018; Pausas et al., 2008; Shakesby, 2011; Shakesby et al., 1996) As a consequence of: (i) a reduction of

evapotranspiration; (ii) a decrease in soil water retention due to hydrophobicity; and (iii) a reduction in obstacles, the likelihood of overland flow is increased, favouring erosion (Shakesby & Doerr, 2006). Also, soil structure may deteriorate after a wildfire by the combustion of soil organic matter (Shakesby & Doerr, 2006), promoting soil erosion (Mataix-Solera et al., 2011). Post-fire erosion is often linked to fire severity (Borrelli et al., 2017; de Vente & Poesen, 2005; Delestre et al., 2017; Foster & Meyer, 1975; Ortíz-Rodríguez et al., 2019; Vieira et al., 2015). In addition, recurrence of multiple wildfires at the same site is perceived to slow down vegetation recovery, increasing runoff, erosion, and nutrient removal (Hosseini et al., 2016; McGuire & Youberg, 2019).

Wildfires are a common threat in Portugal. Mateus and Fernandes (2014) estimated that the accumulated burned area was 4.2×10^6 ha between 1975 and 2012 (~45% of Portugal's land surface), the highest of all southern European countries. Also, Portuguese wildfires had the second largest mean fire size compared to other southern European countries (24.5 ha between 2000 and 2011). Besides an increasing frequency of weather conditions conducive for wildfires (Calheiros et al., 2020), anthropogenic activity such as land use change, induced by socio-economic change and urbanization, also makes an important contribution to wildfire occurrence (Pausas et al., 2008; Shakesby, 2011). In the 20th century in Portugal, part of the agricultural land and shrublands was converted first into Maritime Pine plantations, and towards the end of the century into Eucalypt plantations (Hawtree et al., 2015; Jones et al., 2011; Vasconcelos Ferreira et al., 2010). Initially, the objective of this conversion was to increase the provision of hydrological services such as erosion protection and flood mitigation, however the runoff and erosion increase caused by wildfire disturbances can, in the long run, negate the intended benefits (Carvalho-Santos et al., 2019; Nunes, Naranjo Quintanilla, et al., 2018).

Several studies in north-central Portugal have shown an increase in erosion in burnt areas (Campo et al., 2006; Ferreira et al., 2008; Hosseini et al., 2016; Hyde et al., 2007; Shakesby et al., 1993, 1996). However, these studies mainly focus on short-term processes during a few post-fire years, and on smaller plot or hillslope scales (Shakesby, 2011; Shakesby & Doerr, 2006). Nevertheless, several studies already formulate the need for investigation of the long-term effects, including a consecutive number of wildfires (e.g. McGuire & Youberg, 2019), which could provide insights into the relationship between soil degradation, vegetation change, and other landscape processes that generally occur over a much wider time window. In particular, a better understanding is needed of the importance of occasional severe post-fire erosion events in comparison with long-term background erosion processes (Nunes, Doerr, et al., 2018; Shakesby, 2011; Shakesby & Doerr, 2006). Furthermore, investigating a larger catchment scale can help identify locations with post-fire erosion risk to help delineate intervention strategies, as well as examine the transport pathways of sediments from burnt areas which can have important negative impacts on water quality (Nunes, Bernard-Jannin, et al., 2018, 2020; Shakesby, 2011).

Due to the difficulty of conducting field assessments, numerical modelling studies focusing on the Iberian Peninsula have been conducted to investigate post-fire erosion response. However, these have focused on rather small spatial (patch, hillslope, or small catchment) and temporal (the first few post-fire years) scales (Fernández et al., 2010; Hosseini et al., 2018; Soto & Díaz-Fierros, 1998; Vieira et al., 2015, 2018; Wu, Baartman & Nunes, 2021; Wu et al., 2021; Zema et al., 2020). Models used include the empirical Revised Universal Soil Loss Equation (RUSLE; Fernández & Vega, 2016; Fernández et al., 2010), the semi-empirical Morgan–Morgan–Finney (MMF; Fernández et al., 2010) model, and the physically based Pan-European Soil Erosion Risk Assessment (PESERA; Esteves et al., 2012), Water Erosion Prediction Project (WEPP; Soto & Díaz-Fierros, 1998), and Limburg Soil Erosion Model (OpenLISEM; Wu, Baartman & Nunes, 2021; Wu et al., 2021). Esteves et al. (2012) applied the PESERA model to two headwater catchments (9.7 and 100 ha) for a 50-year simulation period; however, the model only simulated on-site erosion, not accounting for off-site effects caused by sediment transport and deposition. Further studies conducted at the headwater catchment scale (1 km) using LandSoil (Pastor et al., 2019), the Soil and Water Assessment Tool (SWAT; Nunes, Bernard-Jannin, et al., 2018, Nunes, Naranjo Quintanilla, et al., 2018), and OpenLISEM (Wu et al., 2021) show the importance of wildfires for erosion and sediment yield even at longer time scales (20 and 10 years, respectively). However, the complexity of these models—and the large number of parameters required to appropriately simulate post-fire impacts—has limited their applicability with sufficient spatial resolution for larger areas, preventing an analysis of the long-term impacts of recurring wildfires for larger landscapes (>100 km^2), which are typically the units at which forest planning is made. Reduced-complexity landscape evolution models (LEMs) are capable of investigating long-term landscape sediment dynamics (Baartman, van Gorp, et al., 2012; Tucker & Hancock, 2010). Thus, LEMs can be applied to investigate long-term (historical) landscape evolution and sediment behaviour in a wildfire-affected catchment under limited data availability conditions.

The aim of this study was to investigate how multiple wildfires have affected spatial and temporal erosion and deposition dynamics in the Águeda catchment (north-central Portugal, 404 km^2) using a long-term modelling approach. We applied LEM Landscape Process Modelling at Multi-dimensions and Scales (LAPSUS; Schoorl et al., 2000, 2002) to the study area for a 41-year (1979–2020) time period using a wildfire and no-wildfire scenario. In the wildfire scenario, eight major wildfires which occurred in this period were parameterized, with varying severity and spatial extent; while in the no-wildfire scenario, no wildfires were assumed to have taken place. Results were evaluated in terms of (spatially explicit) erosion and deposition rates over time and how these were affected by (1) land use and (2) multiple wildfire occurrence.

2 | METHODS

2.1 | Study area

The Águeda catchment, located in north-central Portugal (40.62° latitude, −8.27° longitude), is commonly affected by wildfires. The catchment covers ~404 km^2 and is situated in the Caramulo mountain formation with peaks of ~1100 m above sea level (Figure 1). Slope steepness ranges between 10 and 25°, with an average of 13.4°. The catchment has a humid Mediterranean climate with annual precipitation of 1000–2500 mm (increasing with altitude), falling mostly in the

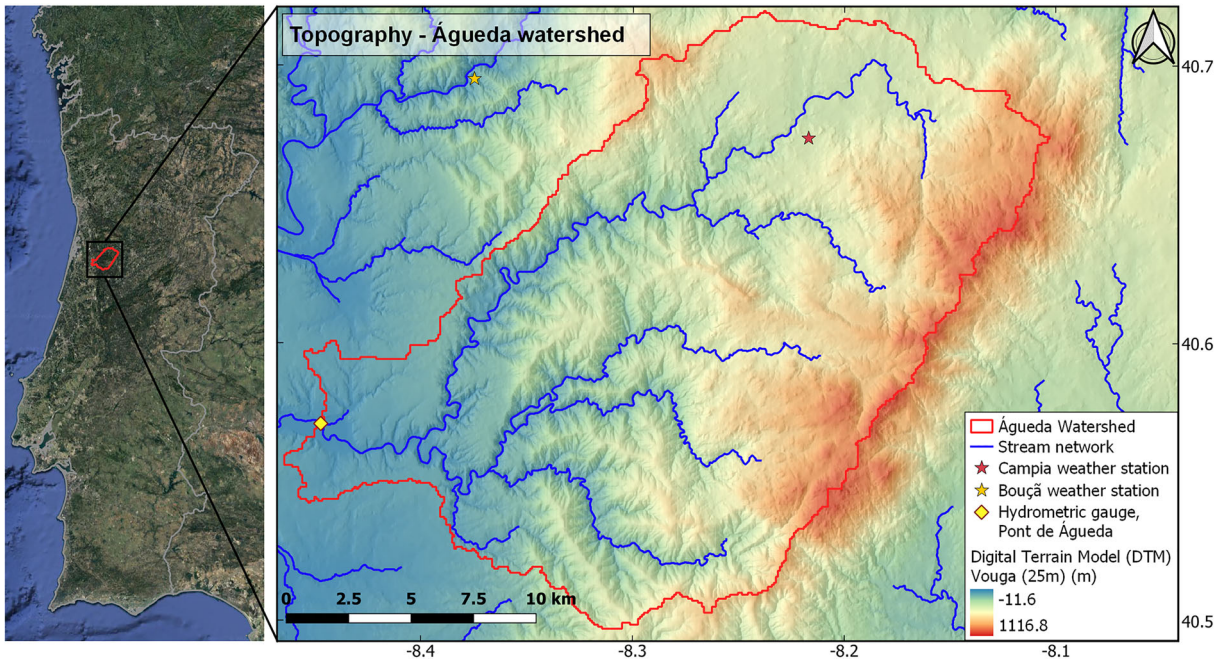

FIGURE 1 Location and topography of the Águeda catchment.

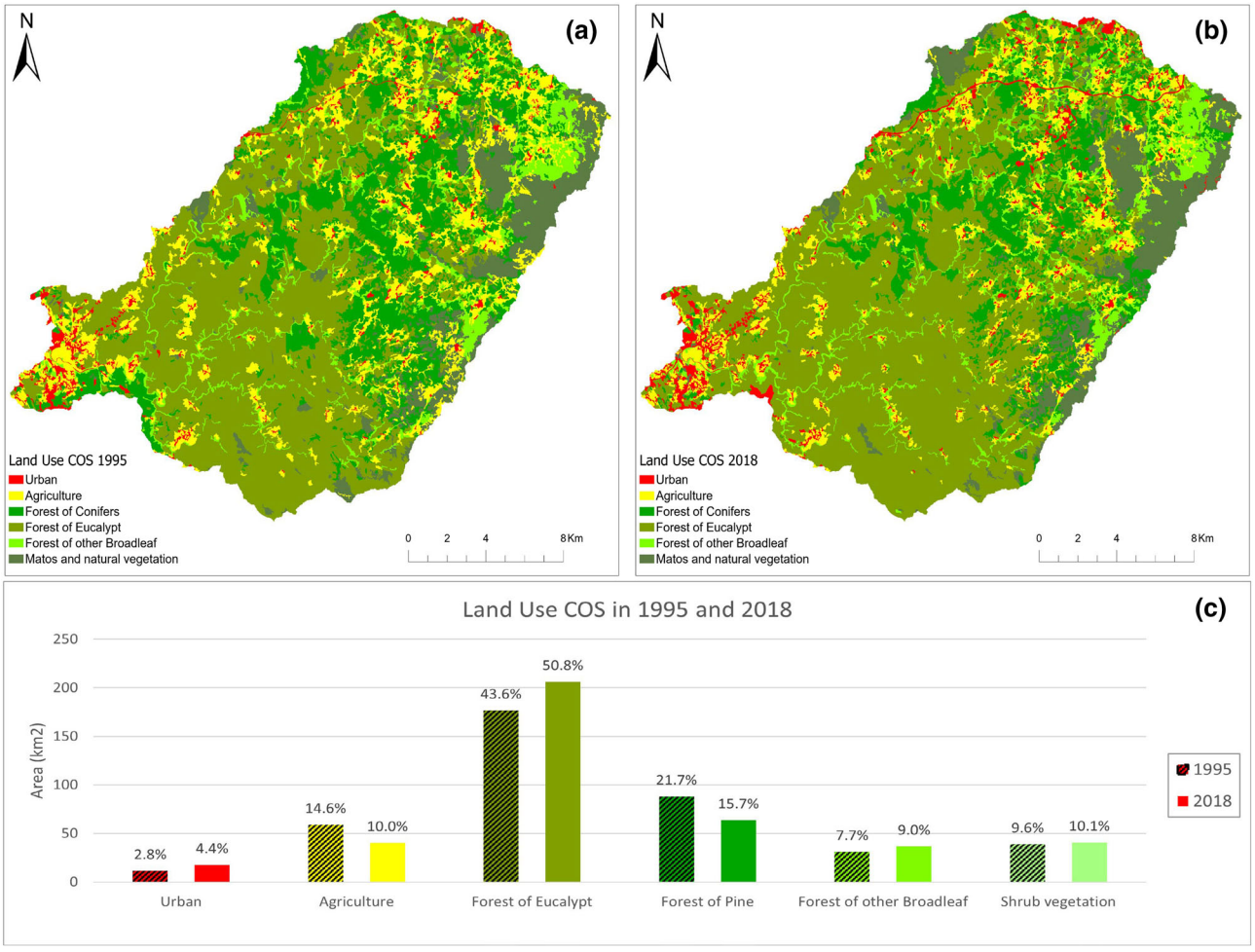

FIGURE 2 Land use in 1995 (a) and 2018 (b) and bar graph (c) showing the percentage cover of each land use type within the catchment (1995: dashed bars, 2018: clear bars). COS is 'carta de Uso e Ocupação do solo'.

autumn and winter months (Hawtree et al., 2015; Nunes, Naranjo Quintanilla, et al., 2018). Mean annual rainfall of 1787 mm was estimated for the period between 1936 and 2010 (Hawtree et al., 2015).

The geology of the Caramulo mountain range is characterized by schist on lower elevations and granites on higher elevated areas (Hawtree et al., 2015; Tavares Wahren et al., 2016). Soil formation in the region generally resulted in shallow soils with low organic matter content and coarse texture properties (Nunes, Naranjo Quintanilla, et al., 2018). Soils are mostly classified as Leptosols between 40 and 75 cm deep, and Cambisols with a depth between 40 and 100 cm (Tavares Wahren et al., 2016; WRB, 2015).

Figure 2 shows the land use in 1995 and 2018, with the percentages for each land use type. Land use evolution (where Pine has been changed for Eucalypt between 1995 and 2018) can be seen, indicating the afforestation practices in the late 20th and beginning 21st century (Ferreira, 1997; Hawtree et al., 2015). Recent recorded major wildfires occurred in 1985, 1986, 1991, 1995, 2005, 2013 (Hawtree et al., 2015), 2016 and 2017. A large wildfire, therefore, took place every ~5 years in the catchment and had a size ranging between 1500 and 9200 ha. Most wildfires occurred during summer (July, August and September), except for the wildfire in 1986 that happened in April.

2.2 | LAPSUS model description

LEM LAPSUS is a physically based model that is able to investigate long-term and large-scale spatial landscape evolution (Baartman, van Gorp, et al., 2012; Schoorl et al., 2000, 2002). The original model includes topography, soil depth, changing land use, climate variability (annual rainfall), and soil and vegetation characteristics (annual quantities as well as spatial evapotranspiration and infiltration) (e.g. Baartman, Temme, et al., 2012); in this study spatial burn severity was also included. Considering the multi-decade timespan of this study, weathering of parent material was not included (Alexander, 1985). Figure 3 shows an overview of the model procedure. Model output consists of annual maps of erosion, deposition, soil depth, and runoff, from which temporal and spatial sediment yield was derived.

LAPSUS is a cellular automata model. Routing of runoff and sediment influx towards neighbouring cells is determined using a multiple flow algorithm based on Holmgren (1994):

$$f_i = \frac{(\Lambda)_i^p}{\sum_{j=1}^{max\ 8} (\Lambda)_j^p} \quad (1)$$

where f_i is the fraction of runoff out of a cell going in direction i (equal to the gradient of the slope Λ in the direction i, powered by the p convergence factor) divided by the total sum of slopes of all lower elevated neighbouring cells j, powered by the factor p.

Incoming water flow Q ($m^2\ yr^{-1}$) for a particular cell equals the incoming water flow (from upslope cells) plus the rainfall on the cell. From this, infiltration and evaporation are subtracted and the remainder is used in the calculation for erosion and deposition and transported to the next (downslope) cell.

For sediment transport, the continuity of transport and conservation of mass principles apply. Equal bulk density of eroded and deposited material is assumed. For each transition from cell to cell along length dx (m) of a finite element, sediment transport capacity C ($m^2\ yr^{-1}$) is calculated (Equation (2)) as a function of fractional discharge Q and slope tangent Λ (Kirkby, 1971):

$$C = \gamma \cdot Q^m \cdot \Lambda^n \quad (2)$$

with discharge exponent m and slope exponent n, and γ a constant for unit conversion with value 1. This is the well-known stream-power equation (Lague, 2014). Transport capacity is compared to the incoming amount of sediment in transport S_0 ($m^2\ yr^{-1}$) to calculate the amount of sediment S ($m^2\ yr^{-1}$) that will be transported:

$$S = C + (S_0 - C) \cdot e^{-dx/h} \quad (3)$$

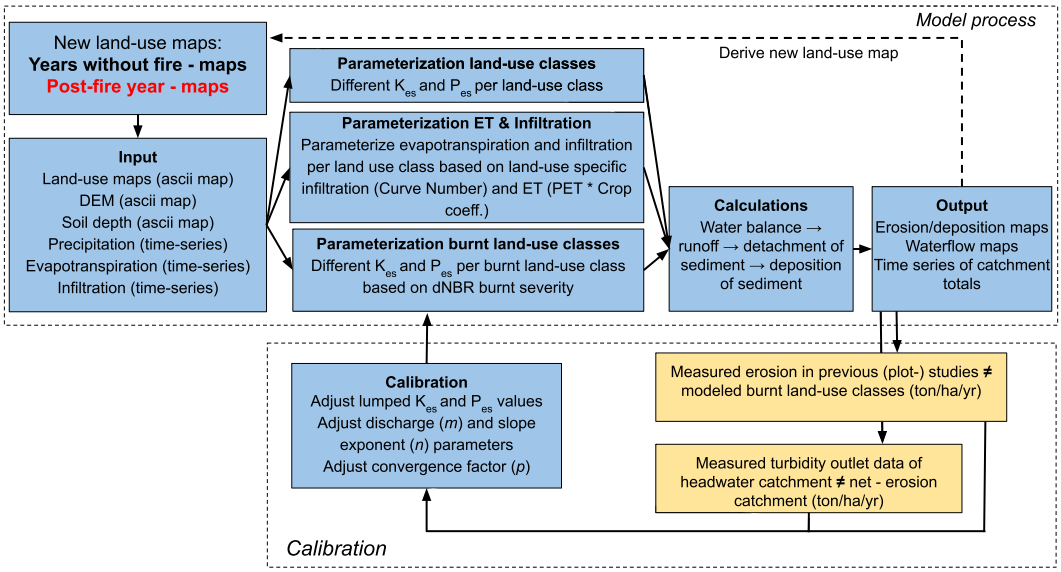

FIGURE 3 Model procedure for LAPSUS showing input data, parameterization, output, and calibration.

with dx the cell size (m). Term h (m) refers to the transport capacity divided by the detachment capacity (D, m yr^{-1}) in case of erosion, and transport capacity divided by settlement capacity (T, m yr^{-1}) in case of sedimentation:

$$D = K_{es} \cdot Q \cdot \Lambda \quad (4)$$

$$T = P_{es} \cdot Q \cdot \Lambda \quad (5)$$

where K_{es} (m^{-1}) is an aggregated surface factor representing the erodibility of the surface, while P_{es} (m^{-1}) is a similar factor for sedimentation potential. The potential for erosion or deposition depends on lumped parameters K_{es} and P_{es}, aggregating different landscape characteristics (vegetation, soil properties, etc.), which are parameterized for different land uses and in this case for burnt areas, both immediately after the wildfire and for the recovery period.

2.3 | Data collection and model parameterization

The main input parameters needed by LAPSUS include a digital elevation model (DEM), land use and soil depth maps, and annual time series of precipitation, evapotranspiration, and infiltration. In this study, a cell size of 25 m and an annual time step were used. The DEM of the Vouga basin was obtained from the Instituto Geográfico do Exército. Soil depth data were based on maps from Tavares Wahren et al. (2016), created using a neural network and soil depth surveys at 11 locations throughout the catchment. The discharge and slope exponents (m and n, respectively; Equation 2) were initially set at 2, based on the work of Kirkby (1987). The initial convergence factor p (Equation 1) was set to 4.0, based on the proposed value in the LAPSUS user guide (van Gorp, 2015).

To analyse the multi-decadal effect of wildfires on erosion, two scenarios were formulated. (i) *Wildfires*: model parameterization accounts for large multiple wildfires (>1000 ha) covering the majority of burnt areas between 1979 and 2020. (ii) *No-wildfires*: wildfires were excluded, thus forming a 'baseline' run. Both scenarios used the same land uses and climate variability (i.e. rainfall, evapotranspiration, and infiltration).

Five land use maps for 1995, 2007, 2010, 2015, and 2018 were used to cover land use change during 41 years (Carta de Uso e Ocupação do Solo [COS] scale: 1:100 000) (see Figure 2 for 1995 and 2018; all years given in Supplementary Material S1). These land use maps were adapted to use a less detailed classification and, for the wildfire scenario, to include the effect of the wildfire in the first, second, and third post-fire years based on burn severity. Only major wildfires >1000 ha were included, which covered ~80% of the total burnt area in the 41-year period considered. These wildfires happened in 1985, 1986, 1991, 1995, 2005, 2013, 2016, and 2017 (Figure 4). Burn severity was estimated by deriving the normalized burn ratio (NBR) using Landsat satellite imagery (ESPA-USGS, 2020), which was used to calculate the different normalized burn ratio (dNBR) by subtracting the pre-fire NBR image from the post-fire NBR image:

$$\mathrm{dNBR} = \mathrm{NBR}_{\mathrm{PRE-FIRE}} - \mathrm{NBR}_{\mathrm{POST-FIRE}} \quad (6)$$

2.3.1 | Erodibility and sediment potential parameterization

The dNBR maps were classified to derive areas of different burn severity (Table 1) and combined with the land use maps. For each land use–burn severity combination, parameterization of lumped K_{es} and P_{es} parameters was based on the USLE vegetation cover factor (USLE_C; Table 2), as vegetation cover is assumed to affect erodibility (i.e. more vegetation cover leads to lower erodibility) and sedimentation potential (i.e. more vegetation cover is assumed to increase sedimentation of transported material). Since LAPSUS does not account for parameterization of the USLE_C value directly, USLE_C values were used as a proxy for fractional change in K_{es} and P_{es} values which are used in the model (Equations 4 and 5). Thus, the absolute value of the USLE_C factor was not used, but the relative differences in USLE_C factors between land use–burn severity combinations (Table 2) were transferred to the K_{es} and P_{es} values for these land

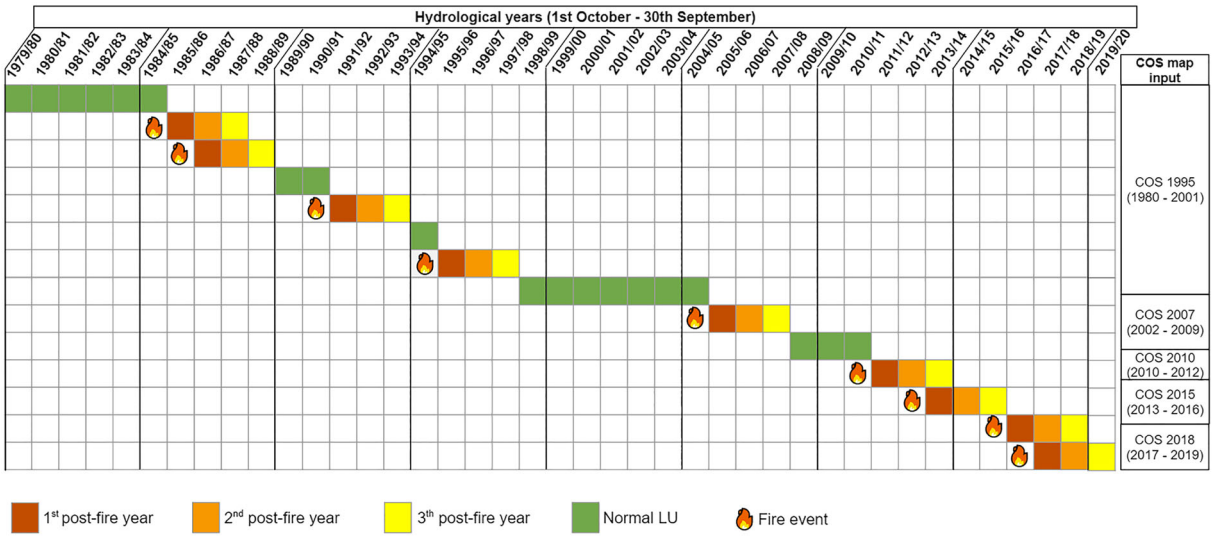

FIGURE 4 Timeline with input land use maps and indication of fire events and post-fire years.

TABLE 1 dNBR intervals for each burn severity class

Burn severity class	dNBR range
Unburnt	−0.1 ≤ dNBR < 0.1
Low severity and regrowth	0.1 ≤ dNBR < 0.27
Moderate severity	0.27 ≤ dNBR < 0.66
High severity	0.66 ≤ dNBR < 1.33

TABLE 2 USLE_C factors for each land use–burn severity class

Land use and burn severity class	USLE_C
Urban	
Unburnt, low, moderate and high severity	5.0×10^{-4}
Agriculture (winter pasture)	
Unburnt	2.0×10^{-3}
Low severity and regrowth	4.4×10^{-3}
Moderate severity	4.5×10^{-2}
High severity	1.832×10^{-1}
Eucalypt, Pine, Other broadleaf forest, Shrub vegetation	
Unburnt	1.0×10^{-3}
Low severity and regrowth	4.4×10^{-3}
Moderate severity	4.5×10^{-2}
High severity	1.832×10^{-1}

use–burn severity combinations. As specific USLE_C data is scarce, a distinction was only made between agriculture, urban, and a combined group of forest (Eucalypt, Pine, other broadleaf forest) and shrub vegetation. For unburnt land uses, USLE_C factors were derived from Nunes, Naranjo Quintanilla, et al. (2018) and were set to 0.001 for the forest/shrub vegetation land uses (Table 2). Urban USLE_C factors were set to be two times lower, due to paved and impermeable conditions of infrastructure and build-up. For agriculture, the value was set at two times higher than the other land uses based on Carvalho-Santos et al. (2016), which simultaneously incorporates the presence of agricultural terraces in the study area. Burn severity was parameterized for each land use (Table 2) based on Fernández and Vega (2016), who identified a power relationship between RUSLE's C-factor and burn severity ($R^2 = 0.77$) at 87 *in-situ* burnt plot measurements in Galicia, Spain.

2.3.2 | Climate data

Total annual quantities of rainfall data for the Áqueda catchment are based on rain gauge weather station data of the 'Campia' station, derived from the 'Sistema Nacional de Informação de Recursos Hídricos' (SNIRH, 2020). Daily totals (mm/day) were transformed to annual totals, resulting in a time series of hydrological years 1979/80 until 2019/20. A hydrological year is set from 1 October to 30 September. Gaps in rainfall data were filled with data from the nearby Bouçã station.

To derive the total annual time series of infiltration and actual evapotranspiration, the catchment outlet streamflow was used. One of the reasons to focus on the Águeda catchment is the availability of the (quite unique) historical daily streamflow data (1936–2012), recorded at the streamflow gauging point 'Ponte de Águeda' at the outlet of the catchment (Hawtree et al., 2015). To derive actual evapotranspiration, the following equation was used:

$$ET_{actual} = P - Q \quad (7)$$

where ET_{actual} is the annual actual evapotranspiration (mm), P is the annual rainfall (m), and Q is the annual streamflow data at the gauging station (mm); deep percolation losses were assumed negligible due to the relatively impermeable geology.

During the dry months (June to September) there were impoundments in the streamflow data due to the closure of a sluice in the river. Missing streamflow or suspicious data from 2004 until 2020 was corrected based on powered regression of streamflow and rainfall data ($R^2 = 0.91$), based on the whole rainfall and streamflow dataset (1936–2012). By using this regression curve, known rainfall values were translated into predicted streamflow values.

To estimate time series of annual infiltration, the concept of baseflow (mm/yr) was used, defined as the fraction of the corrected streamflow data that is not directly generated after a rainfall event in the form of runoff. As this is the lateral flow through the soil column and not the runoff transported over the surface, it therefore serves as a proxy for infiltration. Estimation of baseflow was done by the recursive digital filter method (Arnold et al., 1995; Nathan & McMahon, 1990). This method is considered robust no matter the stream variabilities or catchment size (Nathan & McMahon, 1990).

Apart from including time series data, spatial variability of infiltration and evapotranspiration was included. Differences in actual evapotranspiration (ET_A) values (mm) (shown in Table 3, values without brackets) between land uses were based on multiplication by the potential evapotranspiration (PET), equal for the whole catchment, and the crop coefficient (K_c), different for each land use. For calculation of the PET, the Hargreaves method was used, using monthly temperature variation plus altitude and latitude (Hargreaves & Samani, 1985). For estimation of K_c, an approach from Maselli et al. (2014) was used, that includes seasonality of vegetation cover and soil moisture to account for dry summer months with lower K_c values (see Supplementary Material S2 for an explanatory description about spatial ET).

To estimate spatial variable infiltration values between land uses, the inverse curve number (CN) (Boonstra, 1994; USDA, 2019) was estimated (shown as 'Infiltration' in Table 3, values without brackets). Inverse CNs were determined based on: land use classes (COS classes); soil hydrological groups (4 classes), slope classes (5 classes); the antecedent soil moisture condition (3 classes) and the hydrological condition related to management (3 classes) (Boonstra, 1994). For further explanation of the use of the CN and the parameterization of spatial infiltration, see Supplementary Material S2.

2.4 | Model calibration

To calibrate LAPSUS, the lumped K_{es} and P_{es} factors (Equations 4 and 5) for the whole catchment and the m, n, and p parameters (Equations 1 and 2) were adjusted. Unfortunately, the measured

TABLE 3 Infiltration curve number values and evapotranspiration values (mm) per land use–burn severity combination (values with no brackets); weight factors used in LAPSUS between brackets. A distinction is made between the soil hydrological groups A, B and C, D. For more information, see Supplementary Material S2

	A, B		C, D	
Soil hydrological group	**Infiltration**	**ET_A**	**Infiltration**	**ET_A**
Urban				
Unburnt (unburnt maps)	2.0 (0.092)	147.47 (0.215)	–	–
Unburnt (fire maps)	2.0 (0.032)	147.47 (0.224)	–	–
Low severity and regrowth	2.0 (0.032)	147.47 (0.225)	–	–
Moderate and high severity	2.0 (0.032)	145.84 (0.224)	–	–
Agriculture				
Unburnt (unburnt maps)	68.7 (1.001)	792.72 (1.158)	63.0 (0.918)	792.72 (1.158)
Unburnt (fire maps)	68.7 (1.092)	792.72 (1.207)	63.0 (1.002)	792.72 (1.207)
Low severity and regrowth	35.0 (0.561)	792.72 (1.207)	16.0 (0.257)	792.72 (1.209)
Moderate and high severity	35.0 (0.561)	326.86 (0.499)	16.0 (0.257)	326.86 (0.502)
Eucalypt				
Unburnt (unburnt maps)	78.9 (1.150)	742.12 (1.084)	64.6 (0.942)	742.12 (1.084)
Unburnt (fire maps)	78.9 (1.254)	742.12 (1.130)	64.6 (1.027)	742.12 (1.130)
Low severity and regrowth	35.0 (0.560)	742.12 (1.130)	16.0 (0.255)	742.12 (1.130)
Moderate and high severity	35.0 (0.560)	308.76 (0.472)	16.0 (0.255)	308.76 (0.471)
Pine				
Unburnt (unburnt maps)	78.9 (1.150)	700.76 (1.023)	64.6 (0.942)	700.76 (1.023)
Unburnt (fire maps)	78.9 (1.254)	700.76 (1.067)	64.6 (1.027)	700.76 (1.067)
Low severity and regrowth	35.0 (0.559)	700.76 (1.067)	16.0 (0.256)	700.76 (1.067)
Moderate and high severity	35.0 (0.559)	290.66 (0.444)	16.0 (0.256)	290.66 (0.443)
Other broadleaf forest				
Unburnt (unburnt maps)	81.3 (1.185)	579.47 (0.846)	66.9 (0.975)	579.47 (0.846)
Unburnt (fire maps)	81.3 (1.292)	579.47 (0.882)	66.9 (1.064)	579.47 (0.882)
Low severity and regrowth	35.0 (0.563)	579.47 (0.883)	16.0 (0.258)	579.47 (0.883)
Moderate and high severity	35.0 (0.563)	272.55 (0.417)	16.0 (0.258)	272.55 (0.418)
Shrub vegetation				
Unburnt (unburnt maps)	81.3 (1.185)	538.58 (0.787)	66.9 (0.975)	538.58 (0.787)
Unburnt (fire maps)	81.3 (1.292)	538.58 (0.820)	66.9 (1.064)	538.58 (0.820)
Low severity and regrowth	35.0 (0.561)	538.58 (0.820)	16.0 (0.256)	538.58 (0.820)
Moderate and high severity	35.0 (0.561)	245.40 (0.375)	16.0 (0.256)	245.40 (0.375)

discharge data at the outlet of the Águeda catchment was not suitable to calibrate the annual net erosion simulated by LAPSUS, as it was derived from an uncertain (especially for heavy storms, that carry most sediment) sediment–discharge relation. Therefore, the simulated erosion by LAPSUS was calibrated for a headwater catchment located within the Águeda catchment (i.e. Macieira de Alcôba), which experienced a small fire (~10 ha) in 2011 (Nunes et al., 2020). This smaller headwater catchment contains similar land use, slope, and soil conditions as the Águeda catchment (Nunes, Naranjo Quintanilla, et al., 2018, 2020; Tavares Wahren et al., 2016). Therefore, sediment yields were considered representative for the larger Águeda catchment. Measurements at a burnt hillslope (5.9 ha) (two post-fire years), two agricultural areas (0.63 ha), and 2 min-interval turbidity measurements at a hydrometric station positioned at the outlet (1 pre-fire year and 3 post-fire years) were used to calibrate model outputs (Nunes, Naranjo Quintanilla, et al., 2018, 2020) (see Supplementary Material S3). In addition, plot (8 × 2 m) studies from Shakesby et al. (1996) in the north-west of the Águeda catchment (see Shakesby et al., 1996 for coordinates) and Ferreira (1997) close to Macieira de Alcôba were used to calibrate erosion rates for the unburnt scenario. Because these typical 8 × 2 m bounded plots have limited catchment area, only erosion values in cells in LAPSUS with close to zero flow accumulation were included (<0.228 m^3 for second post-fire year and <0.3 m^3 for third post-fire year). Subsequently, the values included a topographic correction (Supplementary Material S3, values in square brackets), based on Cerdan et al. (2010), so that values are representative for the larger 25 × 25 m cells in LAPSUS. Calibration was done based on the average of multiple (post-fire) years and not for single years, since time-lumped K_{es} and P_{es} factors were used. Supplementary Material S3 lists the observed erosion values, those with topographic correction, and the erosion values as simulated by calibrated LAPSUS.

3 | RESULTS

3.1 | Calibration results

Despite the time-averaged calibration, calibrated model results per year were in all cases of the same order of magnitude as observed data, except for the years 2012/13 and 2013/14 for agricultural slopes in the unburnt scenario: 0.063 vs 0.4 ton ha^{-1} and 1.13 vs 0.44 ton ha^{-1}, respectively. The calibration of all observed values was very good ($R^2 = 0.94$) (Figure 5).

Calibrated values for the model parameter K_{es} and P_{es} factors are given in Table 4. Especially higher P_{es} values were needed to calibrate for the erosion rates in the catchment of Macieira de Alcôba. For the observed values of the burnt scenario, three post-fire years for the outlet (average of 0.19 ton ha^{-1} yr^{-1}) and a relatively high value for the hillslope erosion (average 27.40 ton ha^{-1} yr^{-1}) for the average of two post-fire years could explain the differences between the lower K_{es} and higher P_{es} (Table 4): sediments are deposited before they reach the stream. For the unburnt scenario a similar trend is shown, although K_{es} values were slightly lower. Model parameters m (discharge exponent), n (slope exponent), and p (convergence factor) were adapted to 1.35, 2, and 6, respectively.

3.2 | Effects of wildfires on erosion and sediment deposition

Figure 6a shows the total cumulative erosion and deposition at the end of the 41-year model simulation. Eroded sediments are mostly deposited in larger streams and do not reach the catchment outlet. As soon as valley bottoms start to get wider and slopes become less steep, an increase in sedimentation occurs. However, a gradual decrease of deposition can be seen (e.g. at the lower elevated area in the western part of the catchment; the colour in Figure 6a shifts from

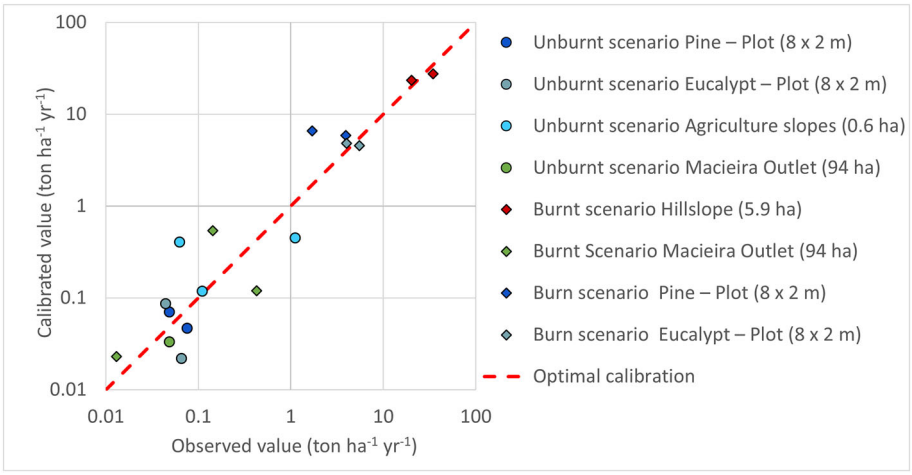

FIGURE 5 Calibrated versus observed erosion values. Red dotted line is 1:1 line.

TABLE 4 Calibrated LAPSUS parameter values

	Burnt scenario		Unburnt scenario	
m = discharge exponent	1.35		1.35	
n = slope exponent	2		2	
p = convergence factor	6		6	
	K_{es}	P_{es}	K_{es}	P_{es}
Lumped K_{es} and P_{es} factor	6.5×10^{-6}	1.0×10^{-1}	4.0×10^{-6}	1.0×10^{-1}
Urban				
Unburnt, low, moderate and high severity	3.25×10^{-6}	5.0×10^{-2}	NA	NA
Unburnt	NA	NA	2.0×10^{-6}	5.0×10^{-2}
Agriculture (winter pasture)				
Unburnt	9.75×10^{-6}	1.5×10^{-1}	2.0×10^{-6}	1.5×10^{-1}
Low severity and regrowth	4.241×10^{-5}	1.5×10^{-1}	NA	NA
Moderate severity	4.3875×10^{-4}	1.5×10^{-1}	NA	NA
High severity	1.78571×10^{-3}	1.5×10^{-1}	NA	NA
Eucalypt, Pine, Other broadleaf forest, Shrub vegetation				
Unburnt	6.5×10^{-6}	1.0×10^{-1}	4.0×10^{-6}	1.0×10^{-1}
Low severity and regrowth	2.828×10^{-5}	1.0×10^{-1}	NA	NA
Moderate severity	2.925×10^{-4}	1.0×10^{-1}	NA	NA
High severity	1.19048×10^{-3}	1.0×10^{-1}	NA	NA

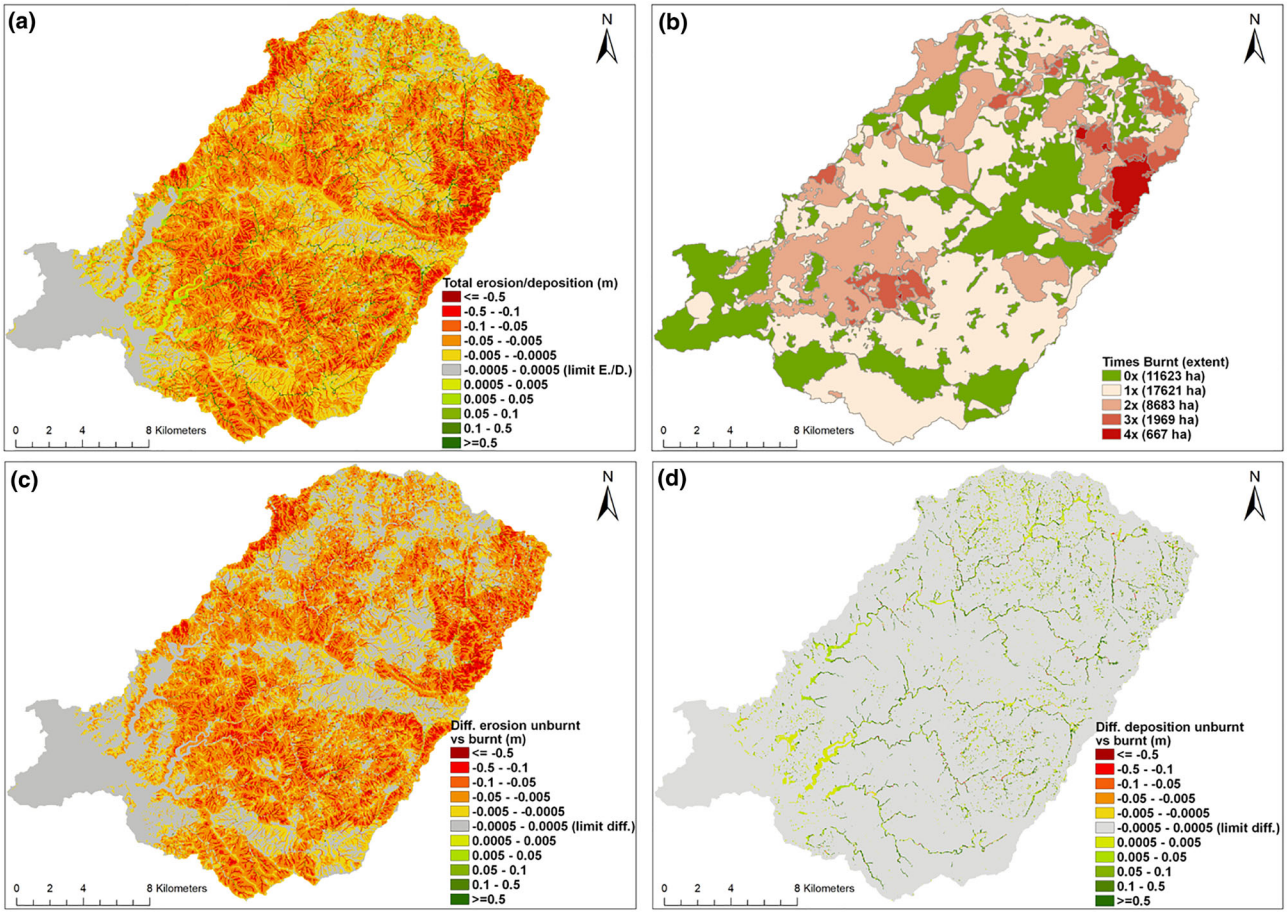

FIGURE 6 (a) Total cumulative erosion and deposition (m) after the 41-year LAPSUS simulation. Note that erosion is given in negative values and deposition in positive values. (b) Fire recurrence based on the dNBR analysis. (c) Difference in total erosion (burnt minus unburnt scenarios). (d) Difference in total deposition (burnt minus unburnt scenarios). For both (c) and (d) red colours implicate an increase in erosion or decrease in deposition, green colours implicate an increase in deposition or a decrease in erosion.

green to yellow at the end of the main streams). The highest erosion rates were simulated in and along the stream network; however, the largest areas with high erosion rates occur in the north-eastern and north-western parts of the catchment, which were the areas with the highest fire frequency (Figure 6b). These are also the areas with the shallower soil types in the catchment, and hence more vulnerable to erosion (Tavares Wahren et al., 2016).

Figures 6c and d show the difference between the burnt and unburnt scenarios for erosion and deposition, respectively, and thus show the potential impact of wildfire on erosion and deposition. Increased erosion due to wildfires is most evident in the central southern area of the catchment and on the catchment borders in the northwest and north-east: locations that exhibited high wildfire recurrence (Figure 6b). These are also the areas which showed higher erosion values. Increased deposition due to wildfires was especially simulated in the main streams (Figure 6d), although there were small spots with lower sedimentation values for the burnt scenario, mostly in locations where several streams merge.

The net erosion simulated by LAPSUS for the burnt scenario was 5.95 ton ha^{-1} yr^{-1} on average, whereas for the unburnt scenario the overall net erosion is one order of magnitude lower: 0.58 ton ha^{-1} yr^{-1}. This is mostly due to much higher values of total erosion for the burnt scenario: 16.26 ton ha^{-1} yr^{-1} for burnt vs 3.46 ton ha^{-1} yr^{-1} for unburnt. There was also an increase in deposition: 10.31 ton ha^{-1} yr^{-1} for burnt vs 2.88 ton ha^{-1} yr^{-1} for unburnt, meaning that a large part of the additional erosion due to wildfire occurrence redeposited downstream, in non-burnt areas. However, the sediment delivery ratio (SDR = net erosion/total erosion) for the burnt scenario was much higher (36.6%) than for the unburnt scenario (16.8%). Thus, more sediment reaches a stream and finally the outlet in a wildfire-affected catchment.

Figure 7a shows the time series of cumulative sediment yield (i.e. net erosion) for all 41 hydrological years in the Águeda catchment, combined with wildfire size and rainfall. Figure 7b shows, for each fire year, the contribution of fire severity in terms of area burned. In general, fire occurrence led to rapid increases of simulated net erosion and total erosion. This increase was particularly evident in the first post-fire year, when compared with the second and third post-fire years.

Model results suggest that the main erosion driver in this region was wildfire occurrence, with rainfall variability as secondary driver. For the unburnt scenario a clear positive relationship between rainfall and erosion rates was found ($R^2 = 0.85$, $p < 0.01$), where for the burnt scenario a positive relationship also existed, but with a weak and not significant correlation ($R^2 = 0.06$, $p > 0.1$; Figure 8). The relatively large extent of (especially) moderate and high burn-severity fires in 2013, 2016, and 2017 (Figure 7b) leads to relatively large increase in net erosion (Figure 7a), except for 2016, which can be explained by 2016 being an exceptionally dry post-fire year. Vice-versa, in 1995 a steep increase in simulated net erosion was simulated (Figure 7a),

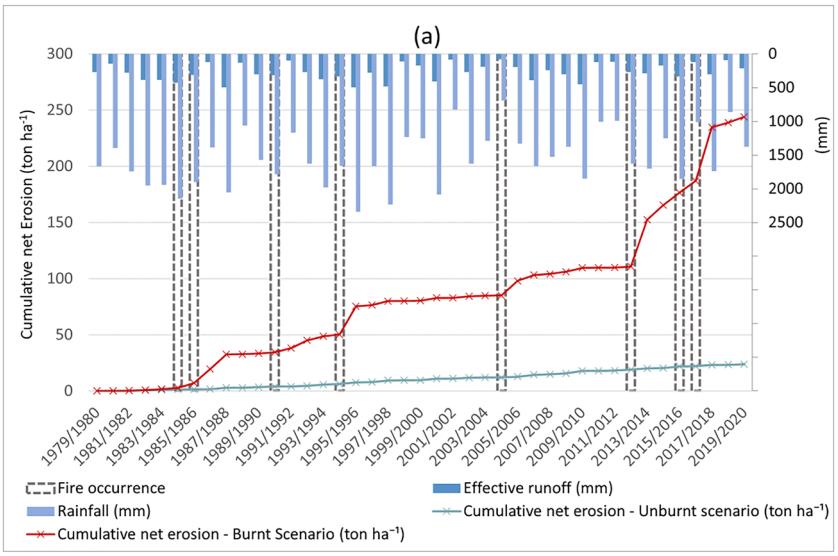

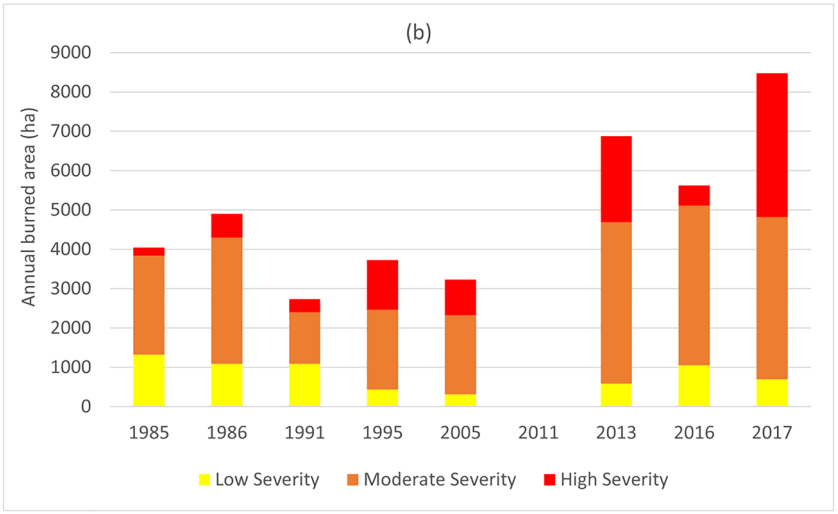

FIGURE 7 (a) Time series of simulated net erosion for the burnt and unburnt scenarios, including rainfall (top blue bars) and fire occurrence (vertical lines). (b) Fire extent (ha) for each fire year, divided into low, moderate, and high severity.

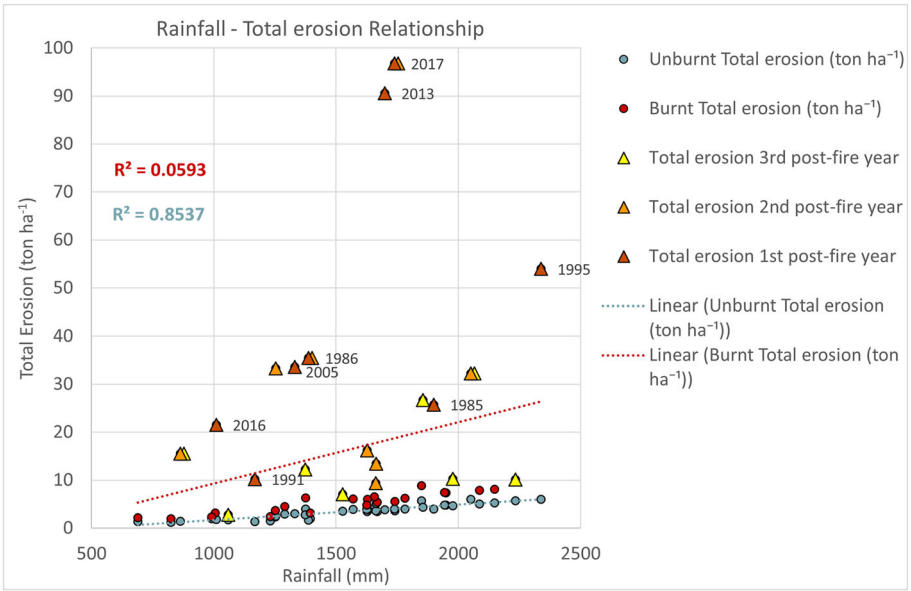

FIGURE 8 Rainfall versus total erosion relationship for the burnt and unburnt scenarios. A weaker correlation for the burnt scenario can be seen, as post-fire years do not follow the trendline.

while the extent of the fire was not so large. This can be explained by 1995 being a very wet post-fire year, still causing relatively much erosion. Thus, primarily fire extent and severity, with in addition rainfall, drive episodes of increased catchment erosion.

3.3 | Spatial patterns of erosion and deposition

For the burnt scenario the land use with the largest contribution to erosion in the catchment was 'Eucalypt' (36.9%; 1.78 ton ha^{-1} yr^{-1}),

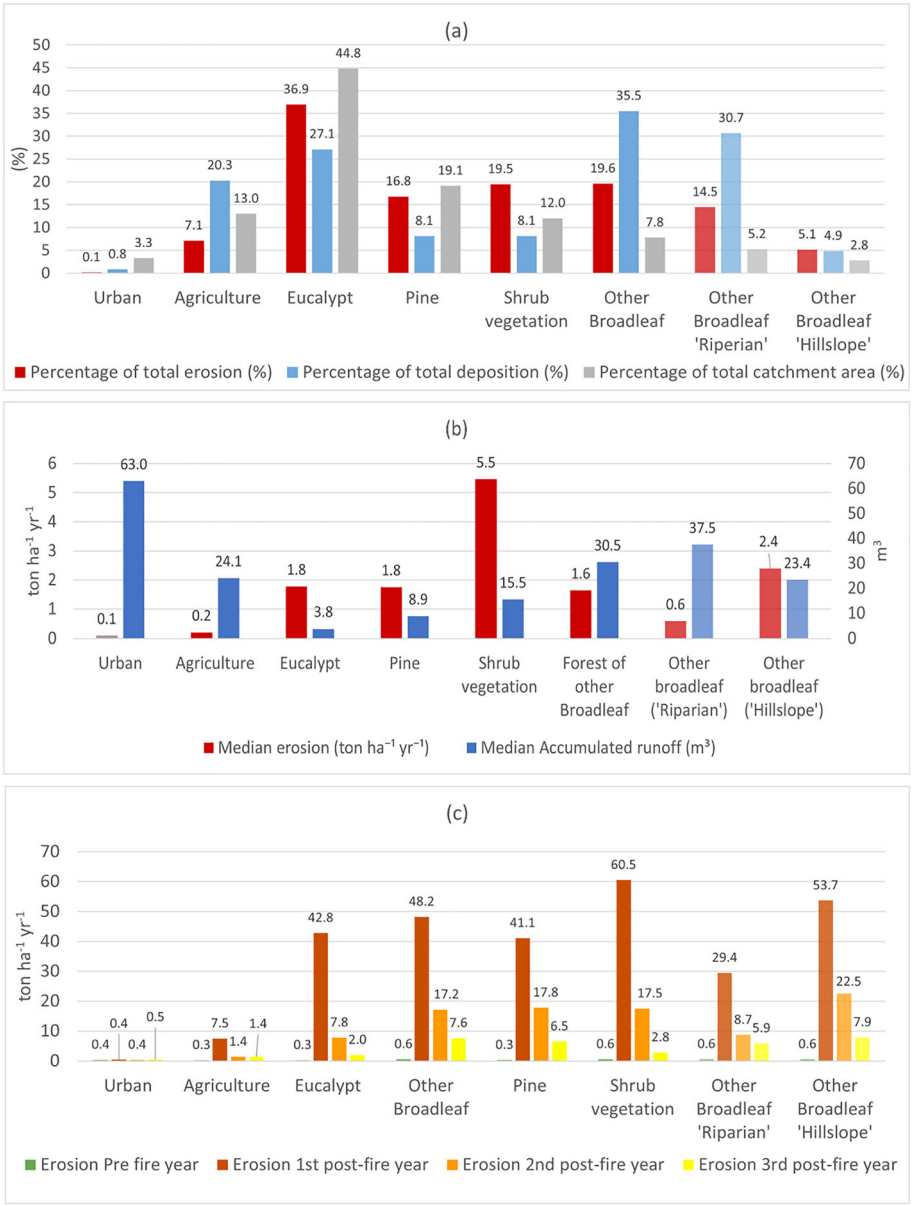

FIGURE 9 (a) Total percentages of erosion (red bars), deposition (blue bars), and percentage of total catchment area per land use (grey bars) for the burnt scenario. (b) Median erosion rates per land use for the burnt scenario (red bars) and median accumulated runoff per land use type, over the 41-year modelled timespan (blue bars). (c) Median erosion rates per land use for the pre-fire year and three post-fire years.

followed by 'Other Broadleaf' (19.6%; 1.64 ton ha^{-1} yr^{-1}), 'Shrubs' (19.5%, 5.46 ton ha^{-1} yr^{-1}), 'Pine' (16.8%, 1.76 ton ha^{-1} yr^{-1}), and 'Agriculture' (7.1%, 0.20 ton ha^{-1} yr^{-1}) (Figures 9a and b). High values for Eucalypt can be associated with a high land occupation (44.8%). By contrast, for 'Shrubs' a low occupation (12.0%) still resulted in a relatively high contribution for erosion (19.5%). An explanation for this is that natural vegetation is twice as often burnt as other vegetation types. Average wildfire recurrences for the 41-year simulation were 0.42, 1.00, 1.08–1.11, and 2.02 times for 'Agriculture', 'Pine', 'Other Broadleaf', 'Eucalypt', and 'Shrubs', respectively.

In addition, the high contribution to erosion of 'Other Broadleaf' (19.6%), but low catchment occupation (7.8%), can be related to broadleaf tree species growing in riparian areas, where localized large erosion rates are caused by channel erosion processes (Figure 9b). To verify this, we analysed the contribution of the 'Other Broadleaf' occurring on hillslopes and the 'Other Broadleaf' occurring in riparian zones separately: 'Other Broadleaf (Riparian)' contributed almost three times more to erosion than 'Other Broadleaf (Hillslope)' (14.5% vs 5.2%) (Figure 9a). For similar reasons, 'Other Broadleaf' contributed to a large extent (35.5%) to the total deposition in the catchment, where especially riparian areas deposited six times more than hillslope areas (30.7% vs 4.9%).

Median erosion rates per land use for the burnt scenario are shown in Figures 9b and c for the 41-year simulation period and only for the post-fire years, respectively. Figure 9b (and to a lesser extent Figure 9c) highlights that median erosion rates are particularly high for 'Other Broadleaf (Hillslope)', 'Shrubs', and to a lesser extent 'Eucalypt' and 'Pine'. This could be linked to the fact that both these landcovers normally had higher burn severity than the others, and also the higher burn frequency of 'Shrubs'. A smaller factor could be the higher runoff values, depicted in Figure 9b (blue bars), and computed as the median runoff per land use type over the 41-year simulation period. Higher values thus mean that more runoff occurs in these land use types, which could contribute to higher erosion rates. The erosion rates show a high variability, as shown by a large difference between the mean and the median, and a high standard deviation and skewness (Table 5). This variability is particularly high for 'Other Broadleaf', again determined by their presence in the riparian area.

TABLE 5 Erosion and deposition rates per land use for areas that encountered different fire recurrences during the 41-year investigation period. The two rightmost columns indicate the standard deviation and skewness per land use

	Mean (median) erosion (ton ha^{-1} yr^{-1})						
	Not burnt	1× burnt	2× burnt	3× burnt	4× burnt	Standard deviation	Skewness
Urban	0.31 (0.10)	0.54 (0.05)	1.33 (0.09)	0.18 (0.00)	2.28 (0.00)	2.44	0.313
Agricultural	2.29 (0.11)	9.12 (0.58)	13.22 (1.84)	16.14 (2.41)	33.49 (7.74)	30.50	0.507
Eucalypt	1.02 (0.19)	10.39 (2.21)	13.60 (3.74)	24.69 (8.02)	15.98 (8.26)	40.44	0.593
Pine	0.75 (0.14)	9.53 (2.42)	21.69 (7.07)	33.32 (10.94)	17.52 (6.54)	42.84	0.615
Shrub vegetation	2.36 (0.57)	12.55 (3.16)	18.88 (5.94)	27.10 (8.80)	43.18 (12.10)	67.53	0.713
Other Broadleaf	5.15 (0.25)	23.84 (2.51)	30.85 (4.62)	40.32 (11.68)	130.25 (21.53)	83.87	0.740
Broadleaf (Riparian)	5.96 (0.23)	28.04 (1.79)	35.39 (1.70)	46.20 (4.79)	229.08 (37.40)	87.04	0.744
Broadleaf (Hillslope)	1.02 (0.28)	10.85 (4.04)	15.18 (8.52)	20.28 (12.68)	27.20 (12.98)	67.48	0.667
	Mean deposition (ton ha^{-1} yr^{-1})						
	No fire	1× burnt	2× burnt	3× burnt	4× burnt	Standard deviation	Skewness
Urban	0.99	0.58	15.88	44.22	34.93	19.16	0.183
Agriculture	7.83	9.67	17.85	6.05	3.60	58.56	0.459
Eucalypt	2.02	3.64	3.20	3.33	0.00	41.20	0.232
Pine	1.61	2.18	2.44	2.93	2.12	28.37	0.223
Shrub vegetation	2.13	2.79	3.93	3.64	3.36	36.68	0.273
Other broadleaf	24.03	20.45	24.21	11.65	4.61	108.17	0.591
Broadleaf (Riparian)	28.47	27.30	33.54	48.45	0.74	126.14	0.678
Broadleaf (Hillslope)	2.08	2.82	8.24	3.09	7.44	46.19	0.271

In addition to this, for all land uses within the first post-fire year, erosion values were generally two orders of magnitude higher than pre-fire erosion rates (Figure 9c) and erosion values generally dropped by ~50% and ~70% in the second and third post-fire years compared to the first post-fire year; this decline was more evident in 'Eucalypt' and 'Shrubs' than in other land covers. This indicates that especially the first post-fire year has the most impact.

Wildfire recurrency also had a large impact on simulated erosion rates. The simulated median erosion rate in almost all land uses was one order of magnitude larger in areas that burnt one or two times compared to areas that did not burn (Table 5). For three or four times burnt areas, the median erosion rates might even be two orders of magnitude higher. For deposition, median values were almost zero, as it was concentrated in small areas. Mean deposition increased with burn frequency for 'Other Broadleaf (Riparian)' and urban areas (i.e. infrastructure), and to a lesser degree for 'Agriculture' until a limit of two times burnt. Note that there was a large variation in the surface area affected by a certain fire recurrence and its related characteristics (e.g. slope steepness).

4 | DISCUSSION

This study investigated the impact of multiple wildfires on erosion patterns over multiple decades in a large catchment (404 km^2). To our knowledge this is the first study investigating post-fire erosion at such a large scale, both spatially and temporally in a Mediterranean country. The results indicate that eight major wildfires in the Águeda catchment during 41 years led to a significant increase in erosion, compared to a situation without wildfire occurrence.

4.1 | Model performance

First of all, model calibration was limited by the scarcity of spatially and temporally explicit measured data. The dataset used for calibration consisted only of plot studies, hillslopes, (unburnt) agricultural slopes, and the headwater catchment of Macieira de Alcôba (94 ha), which is much smaller than the Águeda catchment (404 km^2) (see Supplementary Material S3). Moreover, the few observed years in the dataset made a split-sample approach difficult (i.e. execute both calibration and validation), so that only calibration was possible. This data scarcity is quite common for long-term (historical) time scales and is a problem in many long-term modelling studies (Batista et al., 2019). It is also common in post-fire erosion modelling (Lopes et al., 2021), where the unpredictable occurrence and short nature of wildfire disturbances limits data collection immediately after the wildfire. Nevertheless, both studies emphasize the importance of spatial and temporal data for calibration and validation, and therefore future studies of this nature might focus on areas encompassing a larger number of studies in plots, hillslopes, and small catchments, or where sediment yield data is available.

Furthermore, LAPSUS is an annual-based model that does not include individual storm events. This might be a disadvantage, since sediment yield can be highly variable in space and time and can be dependent on a few single intra-annual rainfall events (Wu, Baartman & Nunes, 2021; Wu et al., 2021) (time compression, as discussed by Smetanová et al., 2019). However, it should be noted that excessive model complexity in the description of temporal patterns might complicate the prediction of long-term erosion patterns due to data scarcity and accumulation of errors; Baartman et al. (2020) stress that model complexity should be adequate to the complexity of the

systems under study. The limited validation and lumped temporal representation make the LAPSUS model results more suitable to show the spatial patterns of erosion and deposition, and give an indication of the order of magnitude of their rates, than to make precise predictions.

Despite these limitations, almost all calibrated erosion rates were of the same order of magnitude as those observed in the Águeda catchment at the plot (Ferreira, 1997; Shakesby et al., 1994) and small catchment scales (Nunes, Doerr, et al., 2018), as shown in Supplementary Material S3 and Figure 5. Furthermore, our results were within the range of multiple Mediterranean plot studies reviewed by Shakesby (2011), although slightly at the 'high end' of observations: the median first post-fire year erosion rates of ~39.2 ton ha^{-1} yr^{-1} in this study fall inside the range 1–50 ton ha^{-1} yr^{-1} for moderate to high burn-severity wildfires, with a median of 3.7 ton ha^{-1} yr^{-1}. Local characteristics of the Águeda catchment could be behind the higher values, especially the higher rainfall compared with other Mediterranean regions, and the large cell sizes of the LAPSUS model (25 × 25 m) compared to the shorter length of typical plot studies.

Moreover, the median long-term erosion rates found in this study for shrublands (5.46 ton ha^{-1} yr^{-1}) correspond with those found in north-west Spain using ^{137}Cs inventories to assess erosion at burnt shrub-covered hillslopes for a 50-year period, ranging from 6.6 to 6.7 ton ha^{-1} yr^{-1} (Menéndez-Duarte et al., 2009). The erosion values found in this study seem therefore to broadly agree with those reported elsewhere in terms of order of magnitude.

It should be noted that the model might also be limited due to the poor representation of several processes in the Águeda catchment; streambank erosion, soil renewal, and tillage erosion could all be relevant. For streambank erosion, the lack of sediment yield data at the catchment scale prevented the determination of different erosivity parameters for streams in LAPSUS (Baartman, van Gorp, et al., 2012), and existing stone walls in streams were not accounted for. Soil renewal was also not accounted for, but it can be argued that these values are negligible at the 41-year time scale due to the low soil renewal rates in the Mediterranean region (around 0.1 ton ha^{-1} yr^{-1} estimated by Alexander, 1985). Finally, tillage in the managed plantation forests of Eucalypt and Pine might be significant due to the short rotation cycles of 10–12 years (Kardell et al., 1986; Shakesby, 2011), estimated at 10 ton ha^{-1} after each treatment in central Portugal (Govers et al., 1996; Shakesby, 2011); again, in the long-term these values are relatively low compared with water erosion, which concurs with the findings of Baartman, Temme, et al. (2012) for millennial time scales.

4.2 | Sediment dynamics at catchment scale

One of the main findings is the high spatial variability of erosion rates, with a high skewness (and a mean one or two orders of magnitude higher than the median) indicating a concentration of erosion in small areas. This can be attributed to different processes operating at different scales, and concurs with the large difference between measurements at the point, plot, or catchment scale mentioned by Shakesby (2011).

The areas of concentrated erosion in the Águeda catchment often have high runoff accumulation, being therefore subjected to gully formation or, at larger scales, streambank erosion (Figure 6a). This concentration of erosion is common to many large catchments, as described for example by de Vente and Poesen (2005) and Smetanová et al. (2019). In burnt areas, topographic features determining runoff concentration overlap with the spatial distribution of wildfire severity to determine erosion 'hotspots', as observed by Fernández et al. (2020), who found a good relation between sediment yield and topographic connectivity modified by burn severity. However, at larger scales, the role of sediment sinks (footslope and floodplain sediment storage) tends to become increasingly important, lowering the sediment yield (de Vente & Poesen, 2005). This has also been proposed for burnt areas by Ferreira et al. (2008), who associated it with a decreasing sediment transport capacity by runoff and streamflow. In the Águeda catchment, LAPSUS indicates that erosion is particularly high in some part of the streams or at locations where streams are originating and the formation of rills, gullies, and streams starts, while deposition occurs particularly in and around the larger streams/rivers (Figure 6a). Model outputs therefore fit within the current knowledge on catchment sediment dynamics.

In general terms, LAPSUS indicates that burnt gullies and streams function as a source of sediment, while footslopes and floodplains function as sinks. Sediments deposited at footslopes and floodplains can subsequently be re-entrained and transported further downstream. Model results indicate that wildfires can change the balance between these factors, as the increase in erosion is larger than the increase in deposition, resulting in a higher sediment delivery ratio and more sediments reaching the outlet.

There is, however, variability in erosion and sediment deposition within the stream network of the Águeda catchment (Figure 6), possibly caused by differences in the connectivity of the stream with upslope locations (Borselli et al., 2008; Heckmann & Schwanghart, 2013). Despite this variability, deposition tends to decrease towards the outlet of the catchment, suggesting a sediment build-up in the larger streams. This process could foster 'sediment cascades' that can behave as 'jerky conveyer belts' towards the stream outlet (Cossart et al., 2018; Schoorl et al., 2014), which has also been observed in other burned catchments (Inbar et al., 1998; Keizer et al., 2015; Mayor et al., 2007).

4.3 | The significance of post-fire erosion in the Águeda catchment

The results indicate that wildfires cause long-term erosion and sediment yield in the Águeda catchment to increase by at least one order of magnitude when compared to natural (i.e. non-disturbed) erosion and sediment yield (Table 5 and Figures 6c and d, 7).

As shown in Figure 8, the relation between rainfall and simulated total erosion was relatively strong, but decreased when wildfires were included in the simulations. This indicates that, when a wildfire occurs, it clearly dominates the effects of rainfall on erosion. This relationship is influenced by wildfire size, and especially burn severity for the fires in 2013 and 2017. When compared with other fires, the larger extent of high burn severity associated with these wildfires corresponds to a larger increase of net erosion, total erosion, and deposition rates for the whole catchment, especially in the first post-fire year (Figure 7). There were relatively high erosion values even in the second and third

post-fire years, which did not occur after smaller and less severe wildfires, which was possibly caused by a slower regeneration of the vegetation or soil (Maia et al., 2012). Interestingly, this difference in sediment processes persists after the wildfire disturbance is negated by vegetation regeneration, as sediment eroded from burnt areas and deposited in the first post-fire years can be available for re-entrainment in years without wildfire-enhanced erosion. This process corresponds to earlier research (Inbar et al., 1998; Mayor et al., 2007; Wittenberg & Inbar, 2009), although in the Águeda headwater catchments Nunes et al. (2020) found that the large rainfall rates can flush these sediments in a few years.

Wildfire-enhanced erosion rates in the Águeda can lead to soil degradation. Median values in pre-fire years are under a tolerable rate of 1 ton ha^{-1} yr^{-1} (Verheijen et al., 2012), but estimated erosion rates for all three years after each fire surpass this threshold by one or two orders of magnitude. Soil depth loss can be especially severe given the generally shallow soils in the Águeda catchment (Tavares Wahren et al., 2016); roughly 8% of the catchment showed a reduction of 10 cm soil depth after 41 years. Moreover, erosion can lead to a decrease in soil fertility (Bakker et al., 2004) through the selective loss of carbon and nutrients (Hosseini et al., 2017; Serpa et al., 2020). Even though our simulated erosion rates are uncertain due to calibration difficulties (see Section 4.1), this concurs with the generally degraded condition of mountain soils in this study area (Tavares Wahren et al., 2016), many of which are already unsuited for Eucalypt plantation and support less profitable Pine plantations. The effects of repeated wildfires on soil quality have also been observed elsewhere in the Mediterranean (Carreira et al., 1996; Hosseini et al., 2016).

Furthermore, the higher connectivity caused by the wildfires can also have implications for water quality. Ashes and fine sediments produced by wildfires can impact ecosystems and limit human uses, due to associated contaminants such as polycyclic aromatic hydrocarbons, heavy metals, and nutrients (Nunes, Naranjo Quintanilla, et al., 2018; Serpa et al., 2020). While the increase in net erosion can indicate potential problems in the immediate years after wildfires, the increase in background sediment concentrations can indicate persistent contamination problems, especially where related to toxic compounds which can be problematic in small amounts and accumulate over time.

4.4 | Contribution of land use to erosion patterns

The results indicate that the most important plantation tree species, Eucalypt and Pine, are the main contributors to the overall sediment budget in the Águeda catchment (Figure 9a). However, mean erosion rates for natural vegetation (predominantly consisting of shrub vegetation) are much higher than those for other species (Table 5 and Figures 9b and c). Several factors contribute to these differences. First, natural vegetation is normally located at the ridges of hills or summits of small mountains, with comparatively shallow soils with lower water-holding capacity (Tavares Wahren et al., 2016) and steeper slopes. Even without wildfire, simulated median erosion rates under natural vegetation are 3 and 4.1 times higher than those of Eucalypt and Pine, respectively (0.57 vs 0.19 and 0.14 ton ha^{-1} yr^{-1}). In addition, shrub areas tend to be more affected by high wildfire severity: 39%, compared with 17% for Eucalypt and 26% for Pine, respectively, making these areas more susceptible to post-fire erosion. This would expose natural vegetation to post-fire erosion more frequently, although it tends to recover faster than other vegetation types: while erosion rates in the second and third post-fire years decreased by 71.1 and 95.4% compared with the first post-fire year, the decrease rates are 56.7/84.2% for Pine and 64.3/84.2% for Other Broadleaf. Eucalypt also seems to recover relatively fast, as rates decrease by 82.8/95.3% in the second and third post-fire years.

Areas with other broadleaf species showed much higher spatial variability, with erosion rates being determined by a low number of cells with relatively high erosion values. This can be explained by the location of part of these forests in riparian areas with higher runoff accumulation, and therefore susceptible to channel bank erosion but also to streambed deposition. This spatial variability is therefore a result of the association between these species and channel processes.

Finally, 'Agriculture' and 'Urban' had lower erosion rates than forest land uses, even though 'Agriculture' is parameterized as more susceptible to erosion (higher K_{es} in Table 4). Note, however, that erosion rates in agricultural land could only be calibrated for unburnt situations, not for burnt situations (see Supplementary Material S3). Agricultural areas are usually located on footslopes, while forests are located on steeper slopes (Tavares Wahren et al., 2016), as is common in most catchments; crop fields located on steeper slopes are usually protected by terraces (Nunes, Bernard-Jannin, et al., 2018). Therefore, even though agriculture is commonly perceived to have a larger impact on erosion (e.g. Cerdan et al., 2010), our results indicate that for the Águeda catchment, high erosion rates predominantly occurred in forest or naturally vegetated areas, thus contradicting the assertion by Shakesby (2011) that in the long-term, erosion rates in burnt Mediterranean areas are below those of croplands.

These results complicate a direct assessment of the land use most responsible for erosion based solely on its characteristics, as the relation between both variables at the Águeda catchment scale seems to be related to wildfire occurrence and recurrence, or their topographic position, rather than local-scale processes such as soil water repellency or soil cover by needle cast (Benito et al., 2003; Shakesby et al., 1994; Walsh et al., 1994). This concurs with the conclusions of Ferreira et al. (2008) that hydrological and sediment connectivity, and their impact by wildfire, drive burnt area erosion response at wider scales.

4.5 | Challenges for land management in the future

Increasing global change could further impact ecosystem services and intensify soil degradation and biodiversity loss, which is detrimental to food and water security (Certini, 2005). In fact, post-fire erosion in the region of north-central Portugal is likely to increase, due to intensified rainfall during the winter months associated with a more intense wildfire regime (Carvalho-Santos et al., 2019; Pastor et al., 2019). Likewise, the wildfires in the last decade (2013, 2016, and 2017) are larger in size and had a larger impact due to higher burn severity. This is partly due to socio-economic drivers such as rural depopulation and (agricultural) land abandonment, leading to encroachment and fostering fuel load build-up, which is perceived to have led to more wildfires (Llovet et al., 2009; Shakesby, 2011).

Areas of natural vegetation were burnt to a larger extent, higher severity, and shorter recurrence times than other forest land uses. However, burnt natural vegetation areas in the north-east of the Águeda catchment received less attention in terms of pre- and post-fire management. Unlike for natural vegetation, plantations have economic value and are therefore better managed, which fits into the ongoing management paradigm to organize and support productive forests and leave natural areas outside the management structure (Shakesby, 2011). Managing natural areas is, however, important to limit wildfire occurrence, soil erosion, and further degradation. Moreover, better management can also decrease toxic or contaminated ashes that are transported downstream (Nunes, Naranjo Quintanilla, et al., 2018). Hence, managing scrub encroachment in the north-east of the Águeda catchment can have positive consequences for natural areas, as well as for downstream areas. Approaches can include low investment options such as prescribed burning to lower the fuel load (Khabarov et al., 2016; Shakesby, 2011), or more conventional but expensive options such as grazing or wildfire breaks (Raftoyannis et al., 2014). Similar options can support managing fuel loads in plantations, together with decreasing tree density (Raftoyannis et al., 2014), although plantation densities in the Águeda are already relatively low. The results of this work can help identify priority management areas and can support post-fire management with emergency post-fire control by mulching (Keizer et al., 2018; Prats et al., 2012), allowing the direction of these measures to areas with greater susceptibility to erosion.

5 | CONCLUSIONS

To the best of our knowledge, this is the first study to quantify post-fire erosion and map sediment transport and deposition patterns at long temporal (41 years) and large spatial (404 km^2) scales. Model calibration was considered good, but lack of data—common in post-fire erosion assessments—limited a full validation of the LAPSUS model. We found that wildfires significantly increased erosion in the Águeda catchment in the last 41 years compared to general background erosion processes by at least one order of magnitude. The first post-fire year had a substantial contribution to erosion, and the post-fire erosion increased with burn severity and wildfire recurrence. Wildfires also amplified the background sediment yield in non-post-fire years, due to the increased availability of sediment build-up in the catchment. Simulated post-fire erosion rates varied spatially, and showed a large skewness, indicating that erosion is concentrated in well-connected areas, either due to topographic or burn severity patterns. Median erosion values were within the range of those reported in the literature for plot studies, although close to the higher end: 5.95 ton ha^{-1} yr^{-1} in the long term, which surpasses a sustainable threshold of 1 ton ha^{-1} yr^{-1}, indicating the potential for long-term soil degradation. While there was differentiation of erosion rates between land uses, this was more related to their topographic position and susceptibility to wildfire (both wildfire severity and recurrence) than their intrinsic characteristics, pointing out the importance of sediment connectivity—and in this case, the changes to connectivity caused by wildfire disturbances—for erosion patterns at larger scales. Finally, we think that due to their spatial outputs, reduced-complexity models such as LAPSUS can function as a tool to identify locations at erosion risk that can be adopted by land managers in pre-fire and post-fire management strategies.

ACKNOWLEDGEMENTS

This work was co-funded by a travel fellowship attributed to D. Follmi through the Erasmus+ programme of the European Union. Additional funding was provided by the Portuguese Foundation for Science and Technology, through project FRISCO (PCIF/MPG/0044/2018), individual grants attributed to J.P. Nunes (IF/00586/2015) and A. Benali (CEECIND/03799/2018/CP1563/CT0003), and the CE3C research centre (UIDB/00329/2020).

AUTHOR CONTRIBUTIONS

Dante Follmi: conceptualization; methodology; investigation (e.g. data collection); writing – initial draft; writing – reviewing and editing. **Jantiene Baartman**: conceptualization; methodology; software (its provision and development); supervision; writing – reviewing and editing. **Akli Benali**: conceptualization; methodology; resources (provision of data, etc.); supervision; writing – reviewing and editing. **Joao Pedro Nunes**: conceptualization; funding acquisition; methodology; resources (provision of data, etc.); supervision; writing – reviewing and editing.

DATA AVAILABILITY STATEMENT

The input and calibration data used in this study is not our own and the source is referred to in the appropriate sections. The output data is presented in maps and tables in the text. We do not intend to share these results further. Interested readers may contact the corresponding author for enquiries.

ORCID

Jantiene Baartman https://orcid.org/0000-0001-6051-8619
Joao Pedro Nunes https://orcid.org/0000-0002-0164-249X

REFERENCES

Alexander, E.B. (1985) Rates of soil formation from bedrock or consolidated sediments. *Physical Geography*, 6(1), 25–42. Available from: https://doi.org/10.1080/02723646.1985.10642261

Arnold, J.G., Allen, P.M., Muttiah, R. & Bernhardt, G. (1995) Automated base flow separation and recession analysis techniques. *Groundwater*, 33(6), 1010–1018. Available from: https://doi.org/10.1111/j.1745-6584.1995.tb00046.x

Baartman, J.E.M., Melsen, L.A., Moore, D. & van der Ploeg, M.J. (2020) On the complexity of model complexity: Viewpoints across the geosciences. *Catena*, 186, 104261. Available from: https://doi.org/10.1016/j.catena.2019.104261

Baartman, J.E.M., Temme, A.J.A.M., Schoorl, J.M., Braakhekke, M.H.A. & Veldkamp, T.A. (2012) Did tillage erosion play a role in millennial scale landscape development? *Earth Surface Processes and Landforms*, 37(15), 1615–1626. Available from: https://doi.org/10.1002/esp.3262

Baartman, J.E.M., van Gorp, W., Temme, A.J.A.M. & Schoorl, J.M. (2012) Modelling sediment dynamics due to hillslope–river interactions: Incorporating fluvial behaviour in landscape evolution model LAPSUS. *Earth Surface Processes and Landforms*, 37(9), 923–935. Available from: https://doi.org/10.1002/esp.3208

Bakker, M.M., Govers, G. & Rounsevell, M.D.A. (2004) The crop productivity–erosion relationship: An analysis based on experimental work. *Catena*, 57(1), 55–76. Available from: https://doi.org/10.1016/j.catena.2003.07.002

Batista, P.V.G., Davies, J., Silva, M.L.N. & Quinton, J.N. (2019) On the evaluation of soil erosion models: Are we doing enough?

Earth-Science Reviews, 197, 102898. Available from: https://doi.org/10.1016/j.earscirev.2019.102898

Benito, E., Santiago, J.L., de Blas, E. & Varela, M.E. (2003) Deforestation of water-repellent soils in Galicia (NW Spain): Effects on surface runoff and erosion under simulated rainfall. *Earth Surface Processes and Landforms*, 28(2), 145–155. Available from: https://doi.org/10.1002/esp.431

Boonstra, J. (1994) Estimating peak runoff rates. In: Ritzema, H.P. (Ed.) *Drainage Principles and Applications*. Wageningen: International Institute for Land Reclamation and Improvement.

Borrelli, P., Robinson, D.A., Fleischer, L.R., Lugato, E., Ballabio, C., Alewell, C. et al. (2017) An assessment of the global impact of 21st century land use change on soil erosion. *Nature Communications*, 8(1), 2013. Available from: https://doi.org/10.1038/s41467-017-02142-7

Borselli, L., Cassi, P. & Torri, D. (2008) Prolegomena to sediment and flow connectivity in the landscape: A GIS and field numerical assessment. *Catena*, 75(3), 268–277. Available from: https://doi.org/10.1016/j.catena.2008.07.006

Calheiros, T., Nunes, J.P. & Pereira, M.G. (2020) Recent evolution of spatial and temporal patterns of burnt areas and fire weather risk in the Iberian Peninsula. *Agricultural and Forest Meteorology*, 287, 107923. Available from: https://doi.org/10.1016/j.agrformet.2020.107923

Campo, J., Andreu, V., Gimeno-García, E., González, O. & Rubio, J.L. (2006) Occurrence of soil erosion after repeated experimental fires in a Mediterranean environment. *Geomorphology*, 82(3-4), 376-387. Available from: https://doi.org/10.1016/j.geomorph.2006.05.014

Carreira, J.A., Arevalo, J.R. & Niell, F.X. (1996) Soil degradation and nutrient availability in fire-prone Mediterranean shrublands of south-eastern Spain. *Arid Soil Research and Rehabilitation*, 10(1), 53–64. Available from: https://doi.org/10.1080/15324989609381420

Carvalho-Santos, C., Marcos, B., Nunes, J., Regos, A., Palazzi, E., Terzago, S. et al. (2019) Hydrological impacts of large fires and future climate: Modeling approach supported by satellite data. *Remote Sensing*, 11(23), 2832. Available from: https://doi.org/10.3390/rs11232832

Carvalho-Santos, C., Nunes, J.P., Monteiro, A.T., Hein, L. & Honrado, J.P. (2016) Assessing the effects of land cover and future climate conditions on the provision of hydrological services in a medium-sized watershed of Portugal. *Hydrological Processes*, 30(5), 720–738. Available from: https://doi.org/10.1002/hyp.10621

Cerdan, O., Govers, G., le Bissonnais, Y., van Oost, K., Poesen, J., Saby, N. et al. (2010) Rates and spatial variations of soil erosion in Europe: A study based on erosion plot data. *Geomorphology*, 122(1), 167–177. Available from: https://doi.org/10.1016/j.geomorph.2010.06.011

Certini, G. (2005) Effects of fire on properties of forest soils: A review. *Oecologia*, 143(1), 1–10. Available from: https://doi.org/10.1007/s00442-004-1788-8

Cossart, E., Viel, V., Lissak, C., Reulier, R., Fressard, M. & Delahaye, D. (2018) How might sediment connectivity change in space and time? *Land Degradation & Development*, 29(8), 2595–2613. Available from: https://doi.org/10.1002/ldr.3022

de Vente, J. & Poesen, J. (2005) Predicting soil erosion and sediment yield at the basin scale: Scale issues and semi-quantitative models. *Earth-Science Reviews*, 71(1), 95–125. Available from: https://doi.org/10.1016/j.earscirev.2005.02.002

Delestre, O., Darboux, F., James, F., Lucas, C., Laguerre, C. & Cordier, S. (2017) FullSWOF: Full shallow-water equations for overland flow. *The Journal of Open Source Software*, 2(20), 448. Available from: https://doi.org/10.21105/joss.00448

ESPA-USGS. (2020) *EROS Science Processing Architecture on Demand Interface*. United States Geological Survey. espa.cr.usgs.gov/ordering/new/

Esteves, T.C.J., Kirkby, M.J., Shakesby, R.A., Ferreira, A.J.D., Soares, J.A.A., Irvine, B.J. et al. (2012) Mitigating land degradation caused by wildfire: Application of the PESERA model to fire-affected sites in Central Portugal. *Geoderma*, 191, 40–50. Available from: https://doi.org/10.1016/j.geoderma.2012.01.001

Fernández, C., Fernández-Alonso, J.M. & Vega, J.A. (2020) Exploring the effect of hydrological connectivity and soil burn severity on sediment yield after wildfire and mulching. *Land Degradation & Development*, 31(13), 1611–1621. Available from: https://doi.org/10.1002/ldr.3539

Fernández, C. & Vega, J.A. (2016) Evaluation of RUSLE and PESERA models for predicting soil erosion losses in the first year after wildfire in NW Spain. *Geoderma*, 273, 64–72. Available from: https://doi.org/10.1016/j.geoderma.2016.03.016

Fernández, C., Vega, J.A. & Vieira, D.C.S. (2010) Assessing soil erosion after fire and rehabilitation treatments in NW Spain: Performance of RUSLE and revised Morgan–Morgan–Finney models. *Land Degradation & Development*, 21(1), 58–67. Available from: https://doi.org/10.1002/ldr.965

Ferreira, A.J.D., Coelho, C.O.A., Ritsema, C.J., Boulet, A.K. & Keizer, J.J. (2008) Soil and water degradation processes in burned areas: Lessons learned from a nested approach. *Catena*, 74(3), 273–285. Available from: https://doi.org/10.1016/j.catena.2008.05.007

Ferreira, C. (1997) Erosão hídrica em solos florestais: estudo em povoamentos de Pinus Pinaster e Eucalyptus Globulus em macieira de Alcôba-Águeda. *Revista da Faculdade de Letras: Geografia*, 13, 145–244.

Foster, G., & Meyer, L. (1975) Mathematical simulation of upland erosion by fundamental erosion mechanics. Present and prospective technology for predicting sediment yields and sources. In *Proceedings of the Sediment-Yield Workshop*, USDA Sedimentation Laboratory, Oxford, MI. Agricultural Research Service, U.S. Department of Agriculture, pp. 190–207.

Govers, G., Quine, T.A., Desmet, P.J.J. & Walling, D.E. (1996) The relative contribution of soil tillage and overland flow erosion to soil redistribution on agricultural land. *Earth Surface Processes and Landforms*, 21(10), 929–946. Available from: https://doi.org/10.1002/(SICI)1096-9837(199610)21:10<929::AID-ESP631>3.0.CO;2-C

Hargreaves, G.H. & Samani, Z.A. (1985) Reference crop evapotranspiration from temperature. *Applied Engineering in Agriculture*, 1(2), 96–99. Available from: https://doi.org/10.13031/2013.26773

Hawtree, D., Nunes, J.P., Keizer, J.J., Jacinto, R., Santos, J., Rial-Rivas, M.E. et al. (2015) Time series analysis of the long-term hydrologic impacts of afforestation in the Águeda watershed of north-central Portugal. *Hydrology and Earth System Sciences*, 19(7), 3033–3045. Available from: https://doi.org/10.5194/hess-19-3033-2015

Heckmann, T. & Schwanghart, W. (2013) Geomorphic coupling and sediment connectivity in an alpine catchment – exploring sediment cascades using graph theory. *Geomorphology*, 182, 89–103. Available from: https://doi.org/10.1016/j.geomorph.2012.10.033

Holmgren, P. (1994) Multiple flow direction algorithms for runoff modelling in grid based elevation models: An empirical evaluation. *Hydrological Processes*, 8(4), 327–334. Available from: https://doi.org/10.1002/hyp.3360080405

Hosseini, M., Geissen, V., González-Pelayo, O., Serpa, D., Machado, A.I., Ritsema, C. et al. (2017) Effects of fire occurrence and recurrence on nitrogen and phosphorus losses by overland flow in maritime pine plantations in north-central Portugal. *Geoderma*, 289, 97–106. Available from: https://doi.org/10.1016/j.geoderma.2016.11.033

Hosseini, M., Keizer, J.J., Pelayo, O.G., Prats, S.A., Ritsema, C. & Geissen, V. (2016) Effect of fire frequency on runoff, soil erosion, and loss of organic matter at the micro-plot scale in north-central Portugal. *Geoderma*, 269, 126–137. Available from: https://doi.org/10.1016/j.geoderma.2016.02.004

Hosseini, M., Nunes, J.P., Pelayo, O.G., Keizer, J.J., Ritsema, C. & Geissen, V. (2018) Developing generalized parameters for post-fire erosion risk assessment using the revised Morgan–Morgan–Finney model: A test for north-central Portuguese pine stands. *Catena*, 165, 358–368. Available from: https://doi.org/10.1016/j.catena.2018.02.019

Hyde, K., Woods, S.W. & Donahue, J. (2007) Predicting gully rejuvenation after wildfire using remotely sensed burn severity data. *Geomorphology*, 86(3-4), 496-511. Available from: https://doi.org/10.1016/j.geomorph.2006.10.012

Inbar, M., Tamir, M. & Wittenberg, L. (1998) Runoff and erosion processes after a forest fire in Mount Carmel, a Mediterranean area. *Geomorphology*, 24(1), 17–33. Available from: https://doi.org/10.1016/S0169-555X(97)00098-6

Jones, N., de Graaff, J., Rodrigo, I. & Duarte, F. (2011) Historical review of land use changes in Portugal (before and after EU integration in 1986) and their implications for land degradation and conservation, with a focus on Centro and Alentejo regions. *Applied Geography*, 31(3), 1036–1048. Available from: https://doi.org/10.1016/j.apgeog.2011.01.024

Kardell, L., Steen, E. & Fabiao, A. (1986) Eucalyptus in Portugal: A threat or a promise? *Ambio*, 15, 6–13.

Keizer, J.J., Martins, M.A.S., Prats, S.A., Faria, S.R., González-Pelayo, O., Machado, A.I. et al. (2015) Within-in flume sediment deposition in a forested catchment following wildfire and post-fire bench terracing, north-central Portugal. *Cuadernos de Investigación Geográfica*, 41(1), 149–164. Available from: https://doi.org/10.18172/cig.2700

Keizer, J.J., Silva, F.C., Vieira, D.C.S., González-Pelayo, O., Campos, I., Vieira, A.M.D. et al. (2018) The effectiveness of two contrasting mulch application rates to reduce post-fire erosion in a Portuguese eucalypt plantation. *Catena*, 169, 21–30. Available from: https://doi.org/10.1016/j.catena.2018.05.029

Khabarov, N., Krasovskii, A., Obersteiner, M., Swart, R., Dosio, A., San-Miguel-Ayanz, J. et al. (2016) Forest fires and adaptation options in Europe. *Regional Environmental Change*, 16(1), 21–30. Available from: https://doi.org/10.1007/s10113-014-0621-0

Kirkby, M. (1971) Hillslope process-response models based on the continuity equation. *Transactions of the Institute of British Geographers*, 3, 15–30.

Kirkby, M. (1987) Modelling some influences of soil erosion, landslides and valley gradient on drainage density and hollow development. *Catena Supplement*, 10, 1–11.

Lague, D. (2014) The stream power river incision model: Evidence, theory and beyond. *Earth Surface Processes and Landforms*, 39(1), 38–61. Available from: https://doi.org/10.1002/esp.3462

Llovet, J., Ruiz-Valera, M., Josa, R. & Vallejo, V.R. (2009) Soil responses to fire in Mediterranean forest landscapes in relation to the previous stage of land abandonment. *International Journal of Wildland Fire*, 18(2), 222–232. Available from: https://doi.org/10.1071/WF07089

Lopes, A.R., Girona-García, A., Corticeiro, S., Martins, R., Keizer, J.J. & Vieira, D.C.S. (2021) What is wrong with post-fire soil erosion modelling? A meta-analysis on current approaches, research gaps, and future directions. *Earth Surface Processes and Landforms*, 46(1), 205–219. Available from: https://doi.org/10.1002/esp.5020

Maia, P., Pausas, J.G., Vasques, A. & Keizer, J.J. (2012) Fire severity as a key factor in post-fire regeneration of *Pinus pinaster* (Ait.) in Central Portugal. *Annals of Forest Science*, 69(4), 489–498. Available from: https://doi.org/10.1007/s13595-012-0203-6

Malvar, M.C., Prats, S.A., Nunes, J.P. & Keizer, J.J. (2011) Post-fire overland flow generation and inter-rill erosion under simulated rainfall in two eucalypt stands in north-central Portugal. *Environmental Research*, 111(2), 222–236. Available from: https://doi.org/10.1016/j.envres.2010.09.003

Maselli, F., Papale, D., Chiesi, M., Matteucci, G., Angeli, L., Raschi, A. & Seufert, G. (2014) Operational monitoring of daily evapotranspiration by the combination of MODIS NDVI and ground meteorological data: Application and evaluation in Central Italy. *Remote Sensing of Environment*, 152, 279–290. Available from: https://doi.org/10.1016/j.rse.2014.06.021

Mataix-Solera, J., Cerdà, A., Arcenegui, V., Jordán, A. & Zavala, L.M. (2011) Fire effects on soil aggregation: A review. *Earth-Science Reviews*, 109(1–2), 44–60. Available from: https://doi.org/10.1016/j.earscirev.2011.08.002

Mateus, P. & Fernandes, P.M. (2014) Forest fires in Portugal: Dynamics, causes and policies. In: Reboredo, F. (Ed.) *Forest Context and Policies in Portugal: Present and Future Challenges*. Cham: Springer International, pp. 97–115.

Mayor, A.G., Bautista, S., Llovet, J. & Bellot, J. (2007) Post-fire hydrological and erosional responses of a Mediterranean landscape: Seven years of catchment-scale dynamics. *Catena*, 71(1), 68–75. Available from: https://doi.org/10.1016/j.catena.2006.10.006

McGuire, L.A. & Youberg, A.M. (2019) Impacts of successive wildfire on soil hydraulic properties: Implications for debris flow hazards and system resilience. *Earth Surface Processes and Landforms*, 44(11), 2236–2250. Available from: https://doi.org/10.1002/esp.4632

Menéndez-Duarte, R., Fernández, S. & Soto, J. (2009) The application of ^{137}Cs to post-fire erosion in north-west Spain. *Geoderma*, 150(1), 54–63. Available from: https://doi.org/10.1016/j.geoderma.2009.01.012

Moriondo, M., Good, P., Durao, R., Bindi, M., Giannakopoulos, C. & Corte-Real, J. (2006) Potential impact of climate change on fire risk in the Mediterranean area. *Climate Research*, 31, 85–95. Available from: https://doi.org/10.3354/cr031085

Nathan, R.J. & McMahon, T.A. (1990) Evaluation of automated techniques for base flow and recession analyses. *Water Resources Research*, 26(7), 1465–1473. Available from: https://doi.org/10.1029/WR026i007p01465

Nunes, J.P., Bernard-Jannin, L., Rodríguez-Blanco, M.L., Boulet, A.K., Santos, J.M. & Keizer, J.J. (2020) Impacts of wildfire and post-fire land management on hydrological and sediment processes in a humid Mediterranean headwater catchment. *Hydrological Processes*, 34(26), 5210–5228. Available from: https://doi.org/10.1002/hyp.13926

Nunes, J.P., Doerr, S.H., Sheridan, G., Neris, J., Santín, C., Emelko, M.B. et al. (2018) Assessing water contamination risk from vegetation fires: Challenges, opportunities and a framework for progress. *Hydrological Processes*, 32(5), 687–694. Available from: https://doi.org/10.1002/hyp.11434

Nunes, J.P., Bernard-Jannin, L., Rodríguez Blanco, M.L., Santos, J.M., Coelho, C.O.A. & Keizer, J.J. (2018) Hydrological and erosion processes in terraced fields: Observations from a humid Mediterranean region in northern Portugal. *Land Degradation & Development*, 29(3), 596–606. Available from: https://doi.org/10.1002/ldr.2550

Nunes, J.P., Naranjo Quintanilla, P., Santos, J.M., Serpa, D., Carvalho-Santos, C. et al. (2018) Afforestation, subsequent forest fires and provision of hydrological services: A model-based analysis for a Mediterranean mountainous catchment. *Land Degradation & Development*, 29(3), 776–788. Available from: https://doi.org/10.1002/ldr.2776

Ortíz-Rodríguez, A.J., Muñoz-Robles, C. & Borselli, L. (2019) Changes in connectivity and hydrological efficiency following wildland fires in Sierra Madre Oriental, Mexico. *Science of the Total Environment*, 655, 112–128. Available from: https://doi.org/10.1016/j.scitotenv.2018.11.236

Pastor, A.V., Nunes, J.P., Ciampalini, R., Koopmans, M., Baartman, J., Huard, F. et al. (2019) Projecting future impacts of global change including fires on soil erosion to anticipate better land management in the forests of NW Portugal. *Water*, 11(12), 122617. Available from: https://doi.org/10.3390/w11122617

Pausas, J.G., Llovet, J., Rodrigo, A. & Vallejo, R. (2008) Are wildfires a disaster in the Mediterranean basin? A review. *International Journal of Wildland Fire*, 17(6), 713–723. Available from: https://doi.org/10.1071/WF07151

Prats, S.A., MacDonald, L.H., Monteiro, M., Ferreira, A.J.D., Coelho, C.O.A. & Keizer, J.J. (2012) Effectiveness of forest residue mulching in reducing post-fire runoff and erosion in a pine and a eucalypt plantation in north-central Portugal. *Geoderma*, 191, 115–124. Available from: https://doi.org/10.1016/j.geoderma.2012.02.009

Raftoyannis, Y., Nocentini, S., Marchi, E., Calama Sainz, R., Garcia Guemes, C., Pilas, I. et al. (2014) Perceptions of forest experts on climate change and fire management in European Mediterranean forests. *iForest – Biogeosciences and Forestry*, 7(1), 33–41. Available from: https://doi.org/10.3832/ifor0817-006

Schoorl, J.M., Sonneveld, M.P.W. & Veldkamp, A. (2000) Three-dimensional landscape process modelling: The effect of DEM resolution. *Earth Surface Processes and Landforms*, 25(9), 1025–1034. Available from: https://doi.org/10.1002/1096-9837(200008)25:9<1025::AID-ESP116>3.0.CO;2-Z

Schoorl, J.M., Temme, A.J.A.M. & Veldkamp, T. (2014) Modelling centennial sediment waves in an eroding landscape – catchment complexity. *Earth Surface Processes and Landforms*, 39(11), 1526–1537. Available from: https://doi.org/10.1002/esp.3605

Schoorl, J.M., Veldkamp, A. & Bouma, J. (2002) Modeling water and soil redistribution in a dynamic landscape context. *Soil Science Society of*

America Journal, 66(5), 1610–1619. Available from: https://doi.org/10.2136/sssaj2002.1610

Serpa, D., Ferreira, R.V., Machado, A.I., Cerqueira, M.A. & Keizer, J.J. (2020) Mid-term post-fire losses of nitrogen and phosphorus by overland flow in two contrasting eucalypt stands in north-central Portugal. *The Science of the Total Environment*, 705, 135843. Available from: https://doi.org/10.1016/j.scitotenv.2019.135843

Shakesby, R.A. (2011) Post-wildfire soil erosion in the Mediterranean: Review and future research directions. *Earth-Science Reviews*, 105(3), 71–100. Available from: https://doi.org/10.1016/j.earscirev.2011.01.001

Shakesby, R.A., Boakes, D.J., Coelho, C.O.A., Gonçalves, A.J.B. & Walsh, R.P.D. (1996) Limiting the soil degradational impacts of wildfire in pine and eucalyptus forests in Portugal: A comparison of alternative post-fire management practices. *Applied Geography*, 16(4), 337–355. Available from: https://doi.org/10.1016/0143-6228(96)00022-7

Shakesby, R.A., Coelho, C.D.A., Ferreira, A.D., Terry, J.P. & Walsh, R.P.D. (1993) Wildfire impacts on soil-erosion and hydrology in wet Mediterranean forest, Portugal. *International Journal of Wildland Fire*, 3(2), 95-110. Available from: https://doi.org/10.1071/WF9930095

Shakesby, R.A., Coelho, C., Ferreira, A.D., Terry, J.P. & Walsh, R.P.D. (1994) Fire, post-burn land management practice and soil erosion response curves in eucalyptus and pine forests, north-central Portugal. In: *Soil Erosion as a consequence of Forest fires*. Logroño, Spain: Geoforma Ediciones, pp. 111–132.

Shakesby, R.A. & Doerr, S.H. (2006) Wildfire as a hydrological and geomorphological agent. *Earth-Science Reviews*, 74(3), 269–307. Available from: https://doi.org/10.1016/j.earscirev.2005.10.006

Smetanová, A., Follain, S., David, M., Ciampalini, R., Raclot, D., Crabit, A. & le Bissonnais, Y. (2019) Landscaping compromises for land degradation neutrality: The case of soil erosion in a Mediterranean agricultural landscape. *Journal of Environmental Management*, 235, 282–292. Available from: https://doi.org/10.1016/j.jenvman.2019.01.063

SNIRH. (2020) *Sistema Nacional de Informação de Recursos Hídricos, Agência Portuguesa do Ambiente*. https://snirh.apambiente.pt/ (last accessed March 2020).

Soto, B. & Díaz-Fierros, F. (1998) Runoff and soil erosion from areas of burnt scrub: Comparison of experimental results with those predicted by the WEPP model. *Catena*, 31(4), 257–270. Available from: https://doi.org/10.1016/S0341-8162(97)00047-7

Tavares Wahren, F., Julich, S., Nunes, J.P., Gonzalez-Pelayo, O., Hawtree, D., Feger, K.H. & Keizer, J.J. (2016) Combining digital soil mapping and hydrological modeling in a data scarce watershed in north-central Portugal. *Geoderma*, 264, 350–362. Available from: https://doi.org/10.1016/j.geoderma.2015.08.023

Tucker, G.E. & Hancock, G.R. (2010) Modelling landscape evolution. *Earth Surface Processes and Landforms*, 35(1), 28–50. Available from: https://doi.org/10.1002/esp.1952

USDA. (2019) *National Engineering Handbook Part 630: Hydrology*. Washington DC: U.S. Department of Agriculture. https://directives.sc.egov.usda.gov/viewerFS.aspx?hid=21422

van Gorp, W. (2015) *LAPSUS User Guide (v0.97) – LAndscape ProcesS modelling at mUlti dimensions and scaleS*. Model Version 5.0.

Vasconcelos Ferreira, R., Azevedo Cerqueira, M., Condesso de Melo, M.T., Rebelo de Figueiredo, D. & Keizer, J.J. (2010) Spatial patterns of surface water quality in the Cértima River basin, Central Portugal. *Journal of Environmental Monitoring: JEM*, 12(1), 189–199. Available from: https://doi.org/10.1039/b914409a

Verheijen, F.G.A., Jones, R.J.A., Rickson, R.J., Smith, C.J., Bastos, A.C., Nunes, J.P. & Keizer, J.J. (2012) Concise overview of European soil erosion research and evaluation. *Acta Agriculturae Scandinavica Section B: Soil and Plant Science*, 62(suppl. 2), 185–190. Available from: https://doi.org/10.1080/09064710.2012.697573

Vieira, D.C.S., Fernández, C., Vega, J.A. & Keizer, J.J. (2015) Does soil burn severity affect the post-fire runoff and interrill erosion response? A review based on meta-analysis of field rainfall simulation data. *Journal of Hydrology*, 523, 452–464. Available from: https://doi.org/10.1016/j.jhydrol.2015.01.071

Vieira, D.C.S., Serpa, D., Nunes, J.P.C., Prats, S.A., Neves, R. & Keizer, J.J. (2018) Predicting the effectiveness of different mulching techniques in reducing post-fire runoff and erosion at plot scale with the RUSLE, MMF and PESERA models. *Environmental Research*, 165, 365–378. Available from: https://doi.org/10.1016/j.envres.2018.04.029

Walsh, R.P.D., Bento-Gonalves, A.J., Boakes, D.J., Coelho, C., Shakesby, R.A., & Thomas, A.D. (1994) Impact of fire-induced water repellency and post-fire forest litter on overland flow in northern and central Portugal. In *Proceedings of the Second International Conference on Forest Fire Research*, vol. II, Coimbra, Portugal, pp. 1149–1159.

Wittenberg, L.E.A. & Inbar, M. (2009) The role of fire disturbance on runoff and erosion processes – a long-term approach, Mt. Carmel case study, Israel. *Geographical Research*, 47(1), 46–56. Available from: https://doi.org/10.1111/j.1745-5871.2008.00554.x

WRB. (2015) *World Reference Base for Soil Resources 2014, update 2015: International soil classification system for naming soils and creating legends for soil maps*. World Soil Resources Reports No. 106. FAO: Rome.

Wu, J., Baartman, J.E.M. & Nunes, J.P. (2021) Testing the impacts of wildfire on hydrological and sediment response using the OpenLISEM model. Part 2: Analyzing the effects of storm return period and extreme events. *Catena*, 207, 105620. Available from: https://doi.org/10.1016/j.catena.2021.105620

Wu, J., Nunes, J.P., Baartman, J.E.M. & Faúndez Urbina, C.A. (2021) Testing the impacts of wildfire on hydrological and sediment response using the OpenLISEM model. Part 1: Calibration and evaluation for a burned Mediterranean forest catchment. *Catena*, 207, 105658. Available from: https://doi.org/10.1016/j.catena.2021.105658

Zema, D.A., Nunes, J.P. & Lucas-Borja, M.E. (2020) Improvement of seasonal runoff and soil loss predictions by the MMF (Morgan–Morgan–Finney) model after wildfire and soil treatment in Mediterranean forest ecosystems. *Catena*, 188, 104415. Available from: https://doi.org/10.1016/j.catena.2019.104415

SUPPORTING INFORMATION

Additional supporting information can be found online in the Supporting Information section at the end of this article.

How to cite this article: Follmi, D., Baartman, J., Benali, A. & Nunes, J.P. (2022) How do large wildfires impact sediment redistribution over multiple decades? *Earth Surface Processes and Landforms*, 1–18. Available from: https://doi.org/10.1002/esp.5441